Development of a method for insect genome editing by adult injection

Yu Shirai

2024

Contents

Chapter 1
General Introduction

With over a million species described, insects are a treasure trove of diversity and represent endless possibilities as research tools for answering fundamental biological questions. Beyond their sheer diversity, a multitude of economically significant species impact areas such as public health and agriculture; therefore, insects are indispensable for ensuring our sustainable existence on earth.

Recent advancements in DNA sequencing and bioinformatics have enabled exploration of comprehensive genomics and transcriptomics in a diverse range of insect species. Concurrently, the significance of targeted genome manipulation has increased, facilitating the understanding of gene functions, genetic networks, and complex biological processes. Genome editing tools such as zinc finger nucleases (ZFNs) (Carroll, 2011), transcription activator-like effector nucleases (TALENs) (Bogdanove and Voytas, 2011), and recently clustered regularly interspaced short palindromic repeats/CRISPR-associated systems (CRISPR/Cas (Jinek et al., 2012), have been developed in recent years. While ZFNs and TALENs require the production of site-specific nucleases through a complex and laborious process, the CRISPR/Cas system utilizes the commonly used nuclease and site-specific single-guide RNAs (sgRNAs) that can be tailored to target specific DNA sequences. Due to its simplicity, the CRISPR/Cas system has been widely used in many animals and plants (Doudna and Charpentier, 2014).

Recent technological improvements in genome editing tools have enabled sophisticated engineering of insect genomes (Gantz and Akbari, 2018; Matthews and Vosshall, 2020). However, the current approaches for insect genome editing require microinjection of

materials into early embryos, which is highly challenging in many insect species as conventional microinjection requires expensive equipment and highly specialized skills (Matthews and Vosshall, 2020; Tamura et al., 2000). Furthermore, accessing the early embryos of many insect species is difficult or almost impossible. For example, cockroaches have an egg case (ootheca) encapsulating the fertilized eggs (e.g., *Blattella germanica*, as shown in Fig. 1.1A); flesh flies give birth to live young ones rather than laying eggs (e.g., *Sarcophaga similis*, as shown in Fig. 1.1B); some stink bug species lay their eggs inside plant tissues (e.g., *Orius strigicollis*, as shown in Fig. 1.1C); and some moth species produce batches of eggs that are covered with hairs and adhesive substances (e.g., *Spodoptera litura*, as shown in Fig. 1.1D). These problems limit the application of genome editing to various groups of insect species.

A new genome editing technology known as Receptor-Mediated Ovary Transduction of Cargo (ReMOT) was developed in 2018 to solve this problem (Chaverra-Rodriguez et al., 2018) (Fig. 1.2). The authors performed genome editing in mosquitoes by injecting Cas9 ribonucleoproteins (RNPs) into the adult females of the yellow fever mosquito *Aedes aegypti*. In this new method, a peptide ligand derived from *Drosophila melanogaster* yolk protein 1 (DmYP1) (P2C ligand), believed to facilitate the translocation of exogenous recombinant proteins into developing oocytes, was fused to the Cas9 protein. As ReMOT can bypass the requirement of microinjection into early embryos, this technology holds great promise and has the potential to become a widely applicable method for insect genome editing.

At the beginning of my Ph.D. work, the use of ReMOT was reported in the mosquito *A. aegypti* (Chaverra-Rodriguez et al., 2018). However, it remained uncertain whether the ReMOT-mediated genome editing approach could be applied to insect species other than *A. aegypti*. Therefore, I attempted to test its applicability to the red flour beetle *Tribolium castaneum* (Chapter 2). As a result, I successfully obtained an edited animal using ReMOT,

although the genome editing efficiency was low. Later, I made a breakthrough by discovering that injection of commercial Cas9 can enable highly efficient genome editing in the German cockroach *Blattella germanica*, and the beetle *T. castaneum*. I named this method "direct parental" CRISPR (DIPA-CRISPR), as mentioned in Chapter 3. Additionally, I demonstrated extended application of DIPA-CRISPR to the knock-in experiments. Finally, I successfully adapted DIPA-CRISPR to the yellow fever mosquito *A. aegypti* (Chapter 4), highlighting the versatility of this method. The results indicated that DIPA-CRISPR has the potential to be used across a wide variety of insects.

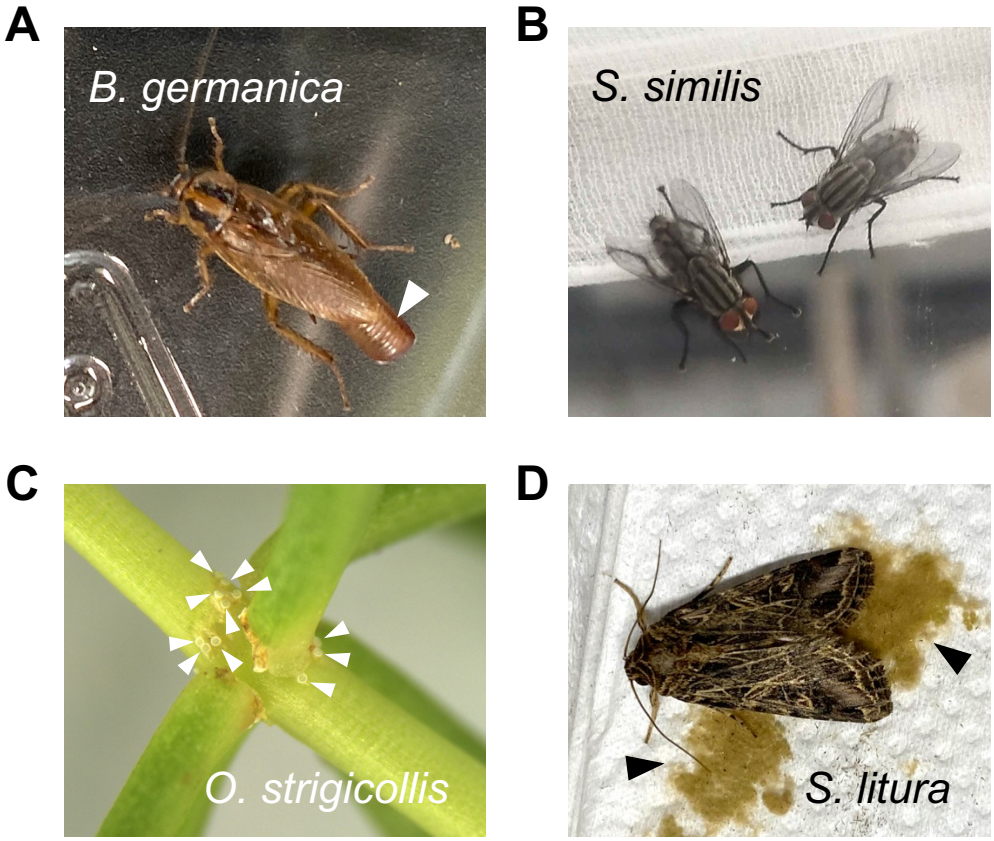

Figure. 1.1. Images of challenging insects for embryonic microinjection

(A) *Blattella germanica* adult female with the ootheca (arrowhead). (B) Adults of *Sarcophaga similis*, which produce live larvae instead of laying eggs. (C) Eggs (arrowheads) of *Orius strigicollis strigicollis* inside plant tissues. (D) *Spodoptera litura* adult female laying batches of eggs (arrowheads) which are covered with hairs and adhesive substances.

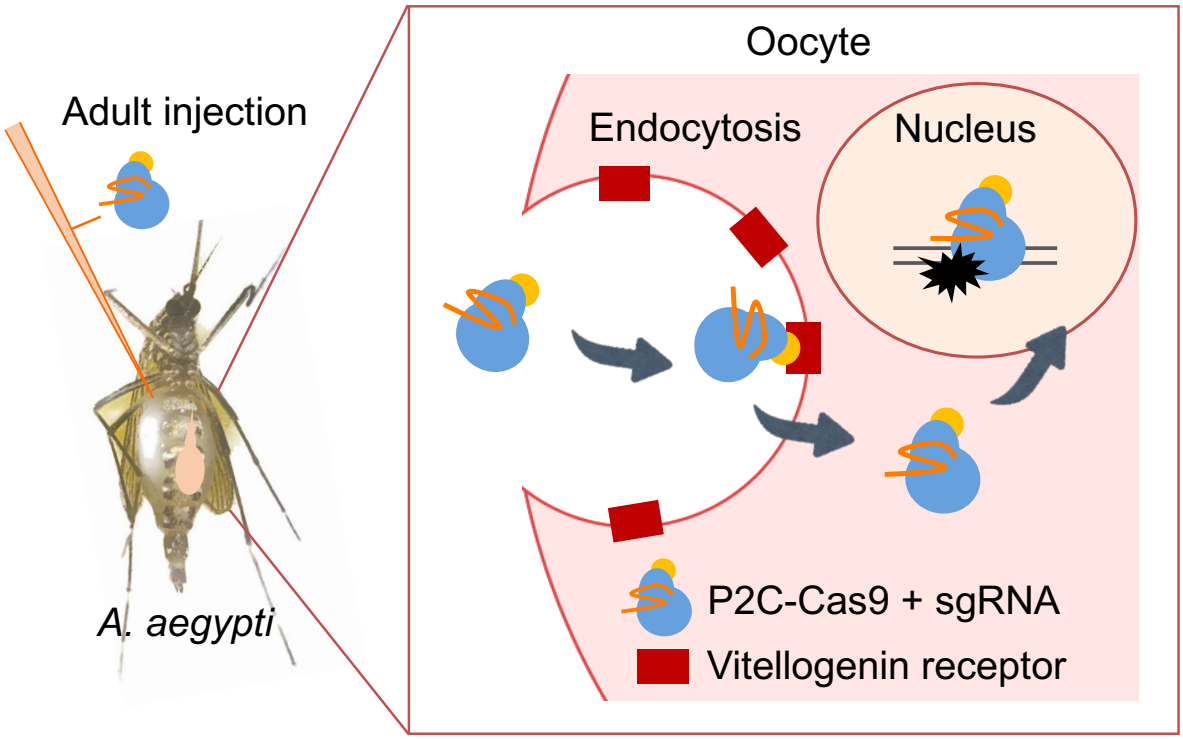

Figure. 1.2. Schematic illustration of ReMOT Control in mosquitoes

Vitellogenic oocytes massively uptake vitellogenins circulating in the hemolymph via receptor-mediated endocytosis. In ReMOT, the peptide ligand P2C likely binds to the vitellogenin receptor, facilitating the incorporation of Cas9 ribonucleoproteins (RNPs) into the endosome of developing oocytes. Then, Cas9 RNPs induce targeted mutagenesis in the nuclei, producing edited G_0 individuals.

References

Bogdanove, A.J., Voytas, D.F., 2011. TAL effectors: Customizable proteins for DNA targeting. Science 333, 1843–1846. https://doi.org/10.1126/science.1204094

Carroll, D., 2011. Genome engineering with zinc-finger nucleases. Genetics 188, 773–782. https://doi.org/10.1534/genetics.111.131433

Chaverra-Rodriguez, D., Macias, V.M., Hughes, G.L., Pujhari, S., Suzuki, Y., Peterson, D.R., Kim, D., McKeand, S., Rasgon, J.L., 2018. Targeted delivery of CRISPR-Cas9 ribonucleoprotein into arthropod ovaries for heritable germline gene editing. Nat. Commun. 9, 1–11. https://doi.org/10.1038/s41467-018-05425-9

Doudna, J.A., Charpentier, E., 2014. The new frontier of genome engineering with CRISPR-Cas9. Science 346, 6213, 1258096. https://doi.org/10.1126/science.1258096

Gantz, V.M., Akbari, O.S., 2018. Gene editing technologies and applications for insects. Curr. Opin. Insect Sci. 28, 66–72. https://doi.org/10.1016/j.cois.2018.05.006

Jinek, M., Chylinski, K., Fonfara, I., Hauer, M., Doudna, J.A., Charpentier, E., 2012. A Programmable dual-RNA-guided DNA endonuclease in adaptive bacterial immunity. Science 337, 816–822.

Matthews, B.J., Vosshall, L.B., 2020. How to turn an organism into a model organism in 10 “easy” steps. J. Exp. Biol. 223, jeb218198. https://doi.org/10.1242/jeb.218198

Tamura, T., Thibert, C., Royer, C., Kanda, T., Abraham, E., Kamba, M., Komoto, N., Thomas, J.L., Mauchamp, B., Chavancy, G., Shirk, P., Fraser, M., Prudhomme, C., Couble, P., 2000. Germline transformation of the silkworm *Bombyx mori* L. using a *piggyBac* transposon-derived vector. Nat. Biotechnol. 18, 559. https://doi.org/10.1038/75446

Chapter 2
ReMOT Control genome editing in beetles

2.1 Introduction

Ommochromes are the major pigments found in the eyes, eggs, wings and epidermis of insects (Figon and Casas, 2019). Research into genes encoding ommochrome biosynthetic enzymes has been conducted over the last four decades using eye color mutants of *Drosophila* and other insects (Figon and Casas, 2019). Tryptophan is the initial precursor of the insect ommochrome biosynthetic pathway. Tryptophan is converted to 3-hydroxykynurenine by a pathway involving tryptophan oxidase, encoded by the *vermilion* gene in *Drosophila*, then kynurenine formamidase, encoded by *kynurenine formamidase* genes, and finally kynurenine 3-hydroxylase, encoded by the *cinnabar* gene (Searles et al., 1990; Searles and Voelker, 1986; Warren, 1996). The resulting 3-hydroxykynurenine is transported into pigment granules by a heterodimer of the half-type ABC transporters White and Scarlet, and is eventually converted to ommochrome pigments such as ommin and xanthommatin (Figon and Casas, 2019; Tatematsu et al., 2011). However, little is known about the final conversion step from 3-hydroxykynurenine to ommochrome pigments (Figon and Casas, 2019).

The red flour beetle *Tribolium castaneum* has long been used as an experimental animal model in genetics and developmental biology, because it is easy to maintain stocks of the beetle, and functions of genes can be readily investigated using approaches such as RNAi and transgenesis (Berghammer et al., 2009; Brown et al., 2009). Many mutant strains have been collected, including eye and body color mutants. This collection of mutants provides a

unique bioresource with which to elucidate the mechanisms of biosynthesis and transport of ommochromes and other pigments, such as melanins and pteridines (Lorenzen et al., 2002). Although there are at least 14 mutant *Tribolium* strains that exhibit altered eye colors (Lorenzen et al., 2002), most of them have not yet been molecularly characterized. Recently, (Osanai-Futahashi et al., 2016) reported that knockdown of the gene *cardinal* in *Tribolium* larvae resulted in a lack of eye pigmentation in pupae and newly emerged adults. The *cardinal* gene is evolutionarily conserved among insects, and encodes a haem peroxidase with a single transmembrane domain. In *Drosophila*, *cardinal* mutants do not have ommochrome pigments in the eyes, but instead accumulate their precursor, 3-hydroxykynurenine (Harris et al., 2011). In the silkworm *Bombyx mori*, *cardinal* mutants [*pink-eyed white egg* (*pe*) mutants in *Bombyx*] have red eyes and white or pale pink eggs instead of the normal dark coloration (Osanai-Futahashi et al., 2016). Biochemical studies have suggested that cardinal catalyzes the last step of ommin formation by using either 3-hydroxykynurenine or xanthommatin as substrates (Figon and Casas, 2019; Osanai-Futahashi et al., 2016).

As the *cardinal* gene in *Tribolium* is located on the X chromosome (Lorenzen et al., 2002; Richards et al., 2008), these results indicate a possibility that *cardinal* is responsible for one of the *Tribolium* eye color mutations known to be linked to the X chromosome. There are two eye color mutant loci on the X chromosome of *Tribolium*: one is the *red-1* locus (Eddleman and Bell, 1963; Lasley, 1960) and the other is the *platinum* locus (Yamada, 1961). The *red-1* locus has four mutant alleles (*red-1*, *peach*, *pink Ndg* and *pink Tiw*) (Lorenzen et al., 2002) and the mutants show variations in eye color from pink to red (Eddleman and Bell, 1963; Lasley, 1960). Conversely, *platinum* mutant adults have white eyes (Yamada, 1961).

In the present study, I identified a gene at the *red-1* locus. Using a candidate gene approach, I found that *red-1* and *peach* mutants have molecular defects in the *cardinal* gene. I also established a novel *cardinal* mutant line using ReMOT (Receptor-Mediated Ovary

Transduction of Cargo) Control-mediated gene knockout (Chaverra-Rodriguez et al., 2018), which was originally developed in mosquitoes. This approach permits maternal or paternal gene disruption without the need for embryo injection. My complementation test demonstrated that *cardinal* is located at the *red-1* locus. My results further suggest that the ReMOT Control-mediated targeted gene disruption can be applicable to beetles.

2.2 Materials and Methods

Insects

Wild type (wt) *Tribolium* culture (Okinawa strain) was obtained from the National Agricultural and Food Research Organization (NARO), Japan. The *red-1* and *peach* strains were kindly provided by the United States Department of Agriculture (USDA). Beetles were reared on wheat flour containing 5% (w/w) brewer's dry yeast at 30˚C and 50–70% relative humidity.

Cloning of *cardinal* genes in mutant strains

Genomic DNA and total RNA were extracted from pupae or adults using DNeasy Blood & Tissue Kits (Qiagen) and TRIzol reagent (Invitrogen), respectively. Genomic PCR and reverse transcription PCR (RT-PCR) were performed using ExTaq DNA polymerase (TaKaRa), using the primers listed in Table 2.1.

RNA interference

To synthesize double-stranded RNA (dsRNA), template DNA was amplified from genomic DNA using specific primers with the T7 promoter sequence added at the 5' end (Table 2.1).

The PCR products were subjected to *in vitro* transcription using the T7 RiboMAX Express Large Scale RNA System (Promega). Approximately 1 µl of the dsRNA solution (2.5 µg/µl) was injected into the dorsal thorax of final or penultimate instar larvae.

Quantitative RT-PCR

Quantitative RT-PCR (qRT-PCR) was performed using the primers listed in Table 2.1, as described previously (Daimon et al., 2015). The relative molarities of the gene transcripts were obtained using crossing point analysis, with standard curves generated using plasmids that contained a fragment of each gene. The expression levels of the target genes were normalized against that of *rp49*.

Expression and purification of recombinant P2C-Cas9 protein

To express the recombinant P2C-Cas9 protein in *E. coli*, an expression vector termed pET24b[P2C-Cas9-His] was constructed. Briefly, a fragment of the *Drosophila yolk protein 1* (*YP1*) gene, which corresponds to the P2C peptide (41 aa) (Chaverra-Rodriguez et al., 2018), was fused to the N-terminus of the Cas9-His cassette in the pET28a-Cas9-His vector (Liang et al., 2017). The fused gene was cloned into the pET24b expression vector (Novagen). An *E. coli* strain, Rosetta2 (DE3) (Novagen), was transformed with pET24b[P2C-Cas9-His], and precultured overnight in Luria Broth (LB) supplemented with 50 µg/ml kanamycin and 34 µg/ml chloramphenicol. Five milliliters of the preculture was added to 1 L of LB medium supplemented with the same antibiotics, and cultured at 16˚C. When the OD_{600} reached 0.5–0.6, 0.1 mM isopropyl ß-D-thiogalactopyranoside was added, and the cells were cultured for 16–20 hours at 16˚C. To extract recombinant P2C-Cas9-His protein, cells were resuspended in 50 ml lysis buffer (50 mM Tris-HCl pH 8.0, 500 mM NaCl, 10 mM imidazole). The suspension was sonicated and centrifuged, and the supernatant was incubated with 1 ml

of Ni Sepharose 6 FF (GE Healthcare). The resin was packed into a gravity-flow column (EconoPack column, Bio-Rad), washed three times with 10 ml of lysis buffer, and eluted with 10 ml of elution buffer (50 mM Tris-HCl pH 8.0, 500 mM NaCl, 500 mM imidazole). Eluted protein was dialyzed in dialysis buffer (50 mM Tris-HCl pH 8.0, 500 mM NaCl) at 4˚C. Protein purity was examined by SDS-PAGE and protein concentration was measured using TaKaRa Bradford Protein Assay Kits (TaKaRa) with bovine serum albumin as a standard.

Synthesis of single-guide RNA

Single-guide RNAs (sgRNAs) that specifically target the *cardinal* gene were designed using the software CRISPRdirect (Naito et al., 2015). To synthesize a large amount of single-guide RNAs, annealed oligo DNA (Table 2.1) was cloned into the BsaI site of the pDR274 vector (Hwang et al., 2013). After linearization with DraI, the vector was used as a template for *in vitro* transcription using the T7 RiboMAX Express Large Scale RNA System (Promega).

***In vitro* cleavage assay**

P2C-Cas9 protein and sgRNA1 (see Fig. 2.1B) were mixed and used to test the cleavage activity of a linearized plasmid into which a fragment of *cardinal* was subcloned. Reactions containing 1 μg of P2C-Cas9, 600 ng of sgRNA1, 250 ng of the linearized plasmid, and 1 x CustSmart buffer (NEB), were incubated for 15 minutes at 37˚C, and the cleavage of the plasmid was visualized by agarose gel electrophoresis followed by staining with ethidium bromide.

Targeted gene disruption of *cardinal* using the ReMOT Control

To disrupt the *cardinal* gene by ReMOT Control (Chaverra-Rodriguez et al., 2018), P2C-Cas9 and two sgRNAs were mixed at a molar ratio of approximately 1 : 2, and incubated for 15

minutes at room temperature to allow ribonucleoprotein (RNP) formation, after which freshly-prepared 70 mM chloroquine was added. Injection was performed using a glass capillary needle equipped with Femtojet 4i (Eppendorf). Female adults (1–2 months after adult emergence; females were thought to have already copulated and started active oviposition by the time of injection) were collected from a stock culture, and injected with ~1 µl of the RNP solution containing 2–3 µg of P2C-Cas9, 1.2–1.5 µg of sgRNAs, and 2 mM chloroquine. Injected female adults (generation zero, G_0) were pooled in a container with wheat flour, and discarded three days after injection. The eye colors of the G_1 animals were examined during pupal and adult stages.

Complementation test

A genetic complementation test was performed to investigate whether a novel mutant *cardinal* allele introduced by ReMOT Control (cd^{ReMOT}) was an allele of the original *red-1* locus. Homozygous cd^{ReMOT}/cd^{ReMOT} virgin females were individually crossed to hemizygous *red-1*/Y or *peach*/Y males (female = XX and male = XY in *Tribolium*), and the eye colors of their offspring were recorded when they reached late pupal stages (pharate adult) or were newly emerged as adults (day 0–1 adult). The eye colors of the F_1 progeny from reciprocal crosses were also recorded.

Primer name	Sequence (5' to 3')	Purpose
Tccd_RT-PCR-F1	TTTGATACCAGCCTCGTACGGGAG	Cloning of *cardinal* (RT-PCR)
Tccd_RT-PCR-R1	AGGGCGCTACAAGGGACGACTTTA	
Tccd_gPCR-F1	TCTTGCGAGAGGGATCAGGTCTTT	Cloning of *cardinal* (genomic PCR of exon 6)
Tccd_gPCR-R1	GGCGTACACCTGCGTATGACG	
Tccd_dsRNA_F1	TAATACGACTCACTATAGGGctccacgatcgcctgttgtg	dsRNA synthesis for *cardinal* RNAi
Tccd_dsRNA_R1	TAATACGACTCACTATAGGGcaagcgctcgtcagcccaat	
Tc_cd_gRNA1-F	TAGGAACAGATGAACCAAGTGA	synthesis of sgRNA1
Tc_cd_gRNA1-R	AAACTCACTTGGTTCATCTGTT	
Tc_cd_gRNA2-F	TAGGCGGTTGGAGGAGAGTCGGAA	synthesis of sgRNA2
Tc_cd_gRNA2-R	AAACTTCCGACTCTCCTCCAACCG	
Tc_v_QF1	TCAGTCAGCCCCACCAAATTCT	qPCR of *vermilion*
Tc_v_QR1	CCCCTGTTCCTAACTGCGAAGA	
Tc_cn_QF1	GCTTTGTCGAACCGTGGCAG	qPCR of *cinnabar*
Tc_cn_QR1	ACATTGTCCCGTTAAAGCATCGT	
Tc_w_QF1	ACTCGAGGCTGCCACTACTG	qPCR of *white*
Tc_w_QR1	CCGCCACAAAACAGCCTTGA	
Tc_st_QF1	TCGCGGATTATGGCAATGCTG	qPCR of *scarlet*
Tc_st_QR1	GCATAAGTGGTGGCACGGAG	
Tc_cd_QF1	CGGTTGGAGGAGAGTCGGAA	qPCR of *cardinal*
Tc_cd_QR1	TGAGTTGTGTTGTCTTGCCCAAA	
TcRp49-QF1	CAGGCACCAGTCTGACCGTTATG	qPCR of *rp49*
TcRp49-QR1	GCTTCGTTTTGGCATTGGAGC	
Tccd_seq_F1	GGCCAAAACCGGGGCGCTTCC	Genotyping of cd^{ReMOT} allele
Tccd_seq_R1	CCGGAAGTTCGTGGGTACAAGCCCG	

Table 2.1. Primers used in this study

2.3 Results

Mutations of *cardinal* in *red-1* and *peach* mutant *Tribolium*

Tribolium red-1 and *peach* mutant adults have white eye colors at eclosion (Fig. 2.1A). These two mutant loci are located on the X chromosome, and belong to the same complementation group (Lorenzen et al., 2002). As the *cardinal* gene is located on the X chromosome (Richards et al., 2008), and adults of *cardinal* RNAi have white eyes (Fig. 2.1A and Osanai-Futahashi et al. 2016), I speculated that *cardinal* is a strong candidate for the gene underlying the *red-1* and *peach* mutations.

To test this hypothesis, I cloned and sequenced cDNAs and genomic DNAs of *cardinal* from *red-1* and *peach* mutants. As shown in Fig. 2.1B, I found molecular defects in *cardinal* in the two mutant lines, which presumably impair the function of the encoded protein. In *red-1*, I found a 1 bp deletion in exon 6 that caused a frameshift mutation (Fig. 2.2). In *peach*, a fragment of a transposable element [~5 kb, 99% identical (in aa) to a putative retrotransposon (XP_015838217)] was inserted into exon 6, which introduced a premature stop codon just after the insertion site (Fig. 2.3). In both alleles, amino acid residues near the C-terminal end of the haem peroxidase domain were mutated. Sequence analysis using PROSITE (https://prosite.expasy.org/) indicated that there is a disulfide bound near the C-terminal end, which is formed by Cys676 and Cys702 (Fig. 2.1B and 2.1C). The latter cysteine residue (Cys702) is missing due to the frameshift mutation in *red-1*, while the premature stop codon is present six amino acid residues downstream of Cys702 in *peach* (Fig. 2.1C), both of which could impair the conformation of cardinal proteins. Collectively, my results strongly suggest that mutations in cardinal are responsible for the *red-1* and *peach* mutations.

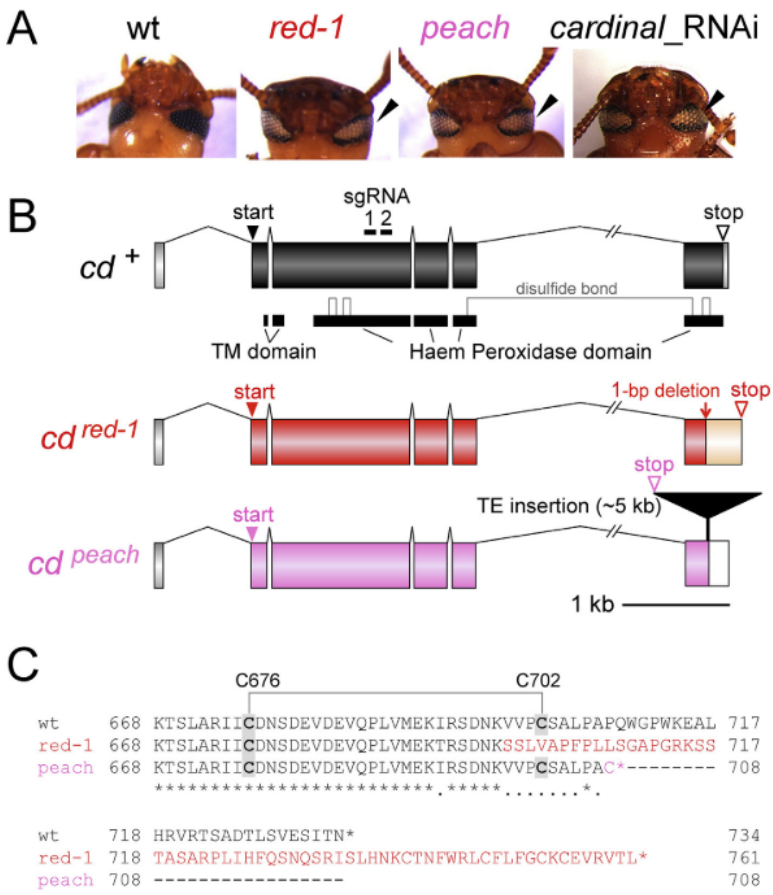

Fig. 2.1. Comparisons of eye colors and cDNA sequences of *cardinal*

(A) Adult eyes of wild type (wt), *red-1,* and *peach Tribolium* strains. The eyes of a *cardinal* RNAi adult are also shown for comparison. Adult eyes were photographed on day 0 (the day of eclosion), and arrowheads indicate the altered eye color phenotypes.

(B) *cardinal* cDNA comparison among wt (cd^{+}, XP_008200769), *red-1* ($cd^{red\text{-}1}$), and *peach* (cd^{peach}) strains. $cd^{red\text{-}1}$ has a 1 bp deletion in exon 6, and cd^{peach} has an insertion of transposable element of around 5 kb in exon 6. Closed and open arrowheads indicate start and stop codons, respectively. Positions of the transmembrane (TM) domain and the haem peroxidase domain are indicated by black lines. Positions of the predicted disulfide bonds are indicated by grey lines. (C) Comparison of amino

acid sequences of cardinal encoded by *wt*, *red-1*, and *peach* alleles. C-terminal sequences of the cardinal proteins (within exon 6) were aligned. Mutated amino acid sequences in *red-1* and *peach* were shown by red and pink letters, respectively. The position of predicted disulfide bond is shown by a grey line, and cysteine residues participating in the disulfide bond (Cys676 and Cys702)are shown by bold letters.

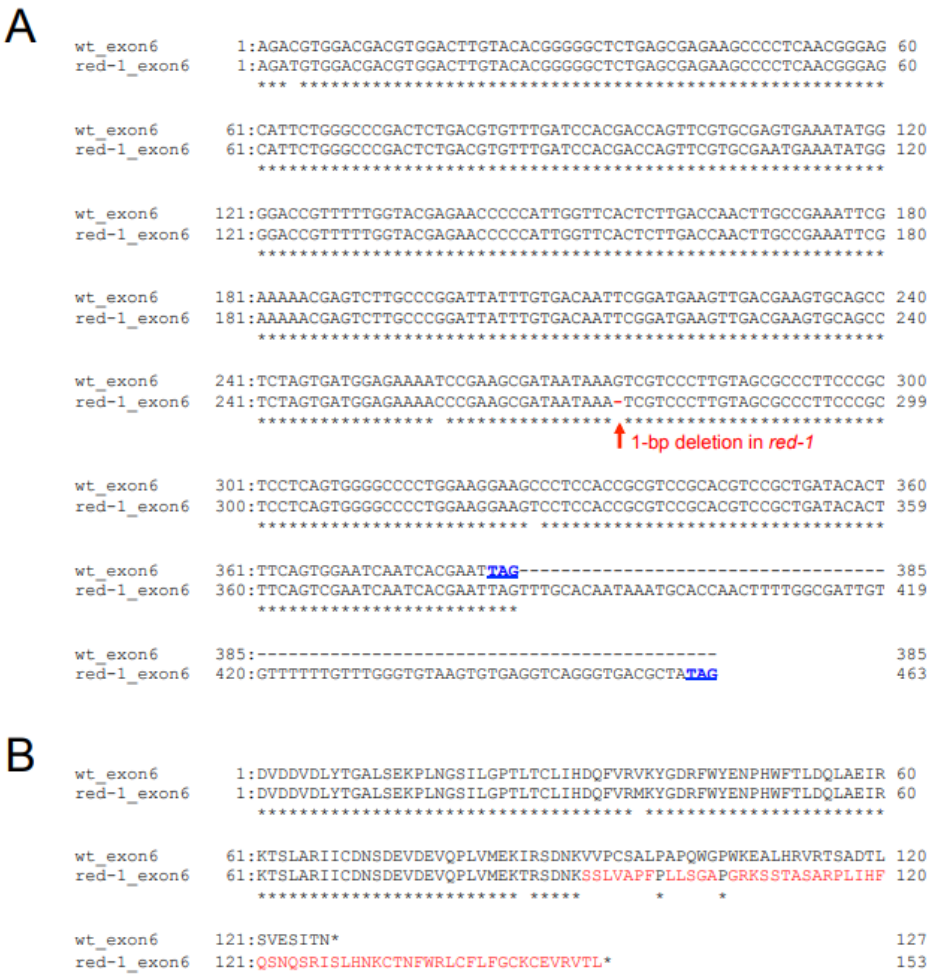

Fig. 2.2. Nucleotide and amino acid sequence of *cardinal* in the *red-1* mutant

(A) Alignment of the nucleotide sequences of exon 6 of cardinal of *wt* and *red-1* strains. Note the presence of a 1 bp deletion in *red-1* allele (shown in red). Stop codons are shown in blue. (B) Alignment of the amino acid sequences of exon 6 of cardinal of *wt* and *red-1* strains. The 1 bp deletion shown in (A) caused a frameshift mutation in *red-1* allele (shown in red letters).

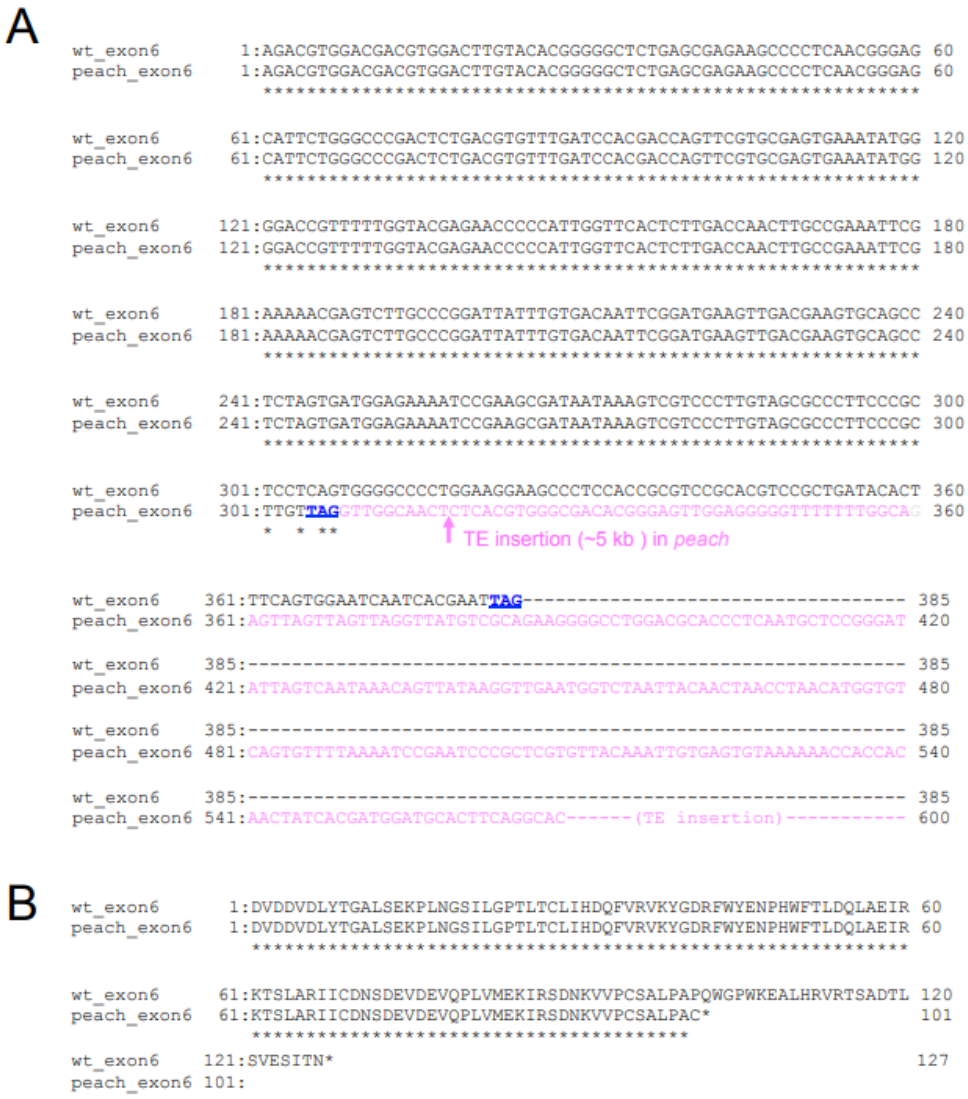

Fig. 2.3. Nucleotide and amino acid sequence of *cardinal* in the *peach* mutant

(A) Alignment of the nucleotide sequences of exon 6 of cardinal of *wt* and *peach* strains. Note that a fragment of the transposable element is inserted in exon 6 of the *peach* allele (shown in pink). Stop codons are shown in blue. (B) Alignment of the amino acid sequences of exon 6 of cardinal of the *wt* and *peach* strains. Insertion of a fragment of the transposable element caused a frameshift mutation (shown in pink letters).

Developmental expression profile of *cardinal*

To further characterize the *cardinal* gene, I investigated the developmental expression profile of *cardinal* and other genes involved in the ommochrome pathway (Fig. 2.4) (Figon and Casas, 2019). As shown in Fig. 2.4A, the pigmentation of compound eyes gradually progresses during the pupal stages, and the eyes are almost fully pigmented by the time of adult eclosion. The expression levels of *vermilion* and *cinnabar* mRNAs gradually increased from pupal day 2 (P2) to adult day 2 (A2). Similarly, the expression levels of *cardinal* gradually increased from P1 and peaked on P5, one day before adult emergence (Fig. 2.4C). On the other hand, *white* and *scarlet* genes, which encode half-type ABC transporters involving in the uptake of the ommochrome pigment precursor 3-hydroxykynurenine from the cytoplasm to pigment granules (Figon and Casas, 2019), appeared to be constitutively expressed during the pupal stages (Fig. 2.4C). Collectively, these results suggest that the expression patterns of the genes encoding the ommochrome biosynthetic enzymes (i.e., *vermilion*, *cinnabar*, and *cardinal*) (Fig. 2.4B) correlate well with the progression of eye pigmentation during pupal stages.

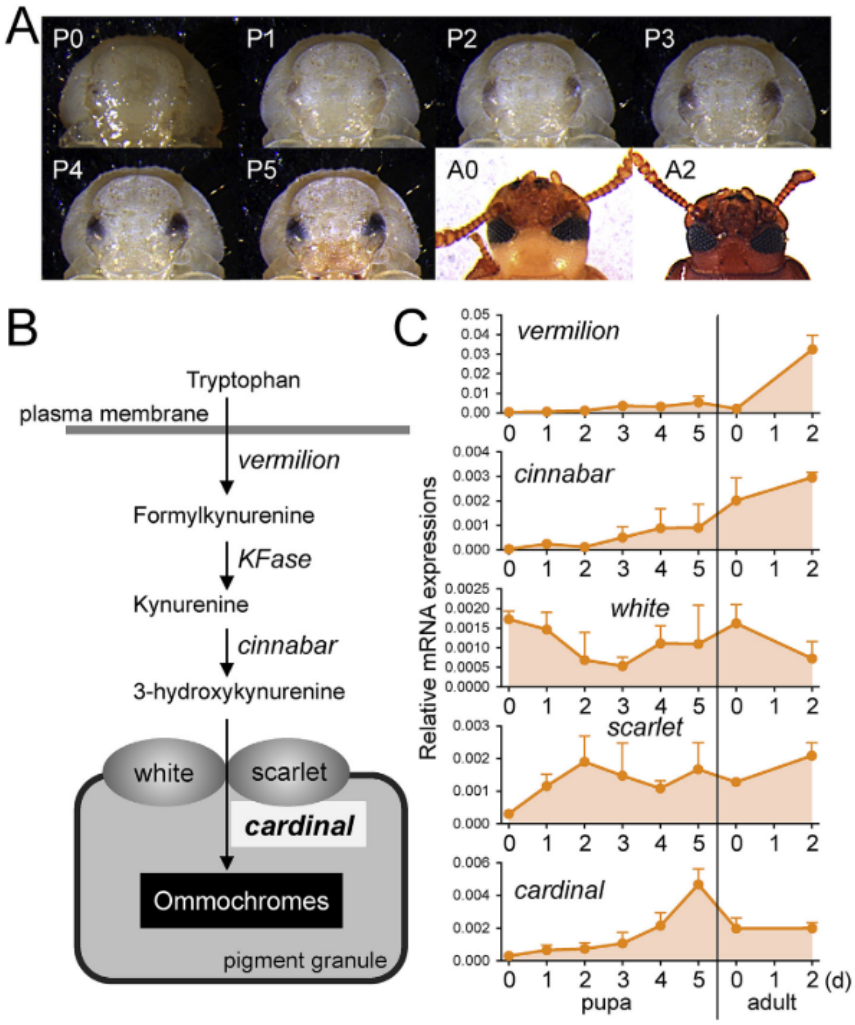

Fig. 2.4. Developmental expression profile of genes involved in ommochrome pathway

(A) Progression of eye pigmentation during pupal and adult stages. Eyes were photographed from pupa day 0 to adult day 2. P0–P5, pupa day 0–5; A0 and A2, adult day 0 and 2. (B) Schematic representation of the ommochrome pathway in *Tribolium*. (C) qRT-PCR analysis of genes involved in ommochrome pathway. Total RNA was extracted from individual whole bodies at each time point. Points indicate mean ± SD (n = 3 biological replicates). The Y-axis indicates the relative mRNA expression levels of each gene normalized against *rp49*. The X-axis indicates developmental stages (d, days) from pupal day 0 to adult day 2.

Targeted mutagenesis of *cardinal* by ReMOT Control

I next performed genome editing experiments to disrupt the *cardinal* gene of the wild type strain (Figs. 2.5 and 2.6). For this experiment, I employed the ReMOT Control technique, which enables maternal and paternal gene disruption by adult injection (Chaverra-Rodriguez et al., 2018). As *cardinal* is located on the X chromosome, I expected that maternal disruption of *cardinal* would yield white-eyed mutant G_1 males (Fig. 2.5A). I expressed and purified recombinant P2C-Cas9 protein (Fig. 2.5B and C), and injected it into female adults together with two single guide RNAs (sgRNAs) targeting *cardinal* (see Fig. 2.1B for the position of the sgRNAs). As shown in Fig. 2.5D, I injected P2C-Cas9 RNP into 55 female adults. Approximately 40% of them died soon after injection, probably due to injection damage, but the remaining 61.8% survived for three days after injection. I screened 383 unsexed G_1 individuals and found one white-eyed individual (Fig. 2.5E, left), which was male, as expected (see Fig. 2.5A). To test whether the *cardinal* gene was mutated in this G_1 male, genomic DNA was extracted from the whole body and used as a template for genotyping PCR. Direct sequencing analysis of the PCR products showed that this G_1 male had a 4 bp deletion in *cardinal*, which was targeted by sgRNA1 (Figs. 2.5F and G, and 2.6). Notably, I did not find any traces of wild type or other mutant alleles in the Sanger electropherogram (Fig. 2.5F). This result indicates that most, if not all, of the somatic and germline cells of this animal carried the same 4 bp deletion. Therefore, it is likely that the 4 bp deletion was introduced into the oocyte of a G_0 female during oogenesis. I also performed control experiments using non-tagged Cas9 (Cas9 without the P2C ligand), but I did not recover any white-eyed animals. This result suggests that the P2C ligand facilitated the uptake of Cas9 RNP from hemolymph to oocytes.

To test whether the novel mutation introduced by ReMOT Control (cd^{ReMOT}) could be inherited in an X-linked manner, the G_1 mutant male was crossed with wild type virgin

females. As shown in Table 2.2, all of the F_1 offspring had normal black eyes (+/Y males and cd^{ReMOT}/+ females). When the F_1 females were backcrossed to wild type males, approximately half of the male progeny had white eyes (cd^{ReMOT}/Y), demonstrating that the cd^{ReMOT} allele can be inherited in an X-linked manner. I did not find any apparent abnormalities in development, fecundity, or morphology in cd^{ReMOT} animals, except for the eye colors.

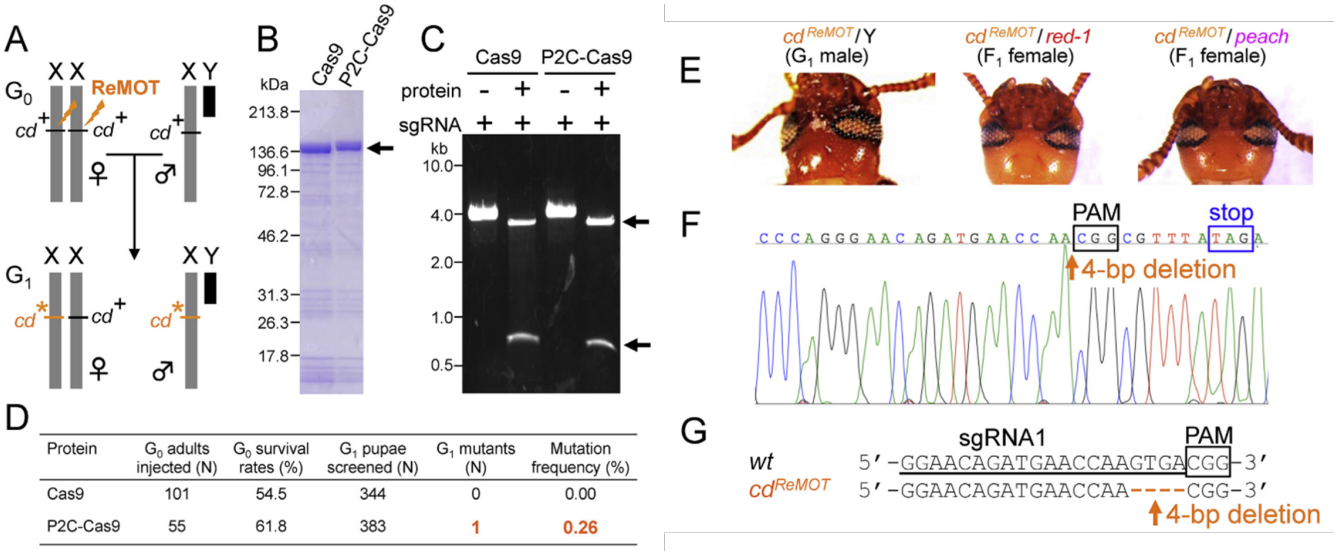

Protein	G_0 adults injected (N)	G_0 survival rates (%)	G_1 pupae screened (N)	G_1 mutants (N)	Mutation frequency (%)
Cas9	101	54.5	344	0	0.00
P2C-Cas9	55	61.8	383	1	0.26

Fig. 2.5. ReMOT Control-mediated targeted disruption of *cardinal*

(A) A scheme for ReMOT Control-mediated disruption of *cardinal*. Females are XX and males are XY in *Tribolium*. Therefore, if a recessive *cardinal* mutation is introduced into a maternal allele by ReMOT Control (upper panel, shown in orange), the resultant mutant allele (cd^*) would be inherited by the G_1 (lower panel) and the phenotype would be manifested in hemizygous G_1 males. (B) CBB staining of purified Cas9 and P2C-Cas9 recombinant proteins. Bands for Cas9 and P2C-Cas9 are indicated by an arrow, and the sizes of the molecular markers are shown on the left. (C) *In vitro* cleavage assay of Cas9 and P2C-Cas9. sgRNA1 was incubated with Cas9 or P2C-Cas9, and the resultant RNPs were tested for the cleavage activity of a linearized plasmid. Cleaved DNA fragments are indicated by arrows, and sizes of DNA markers are shown on the left. (D) Summary of ReMOT Control experiments. Cas9 or P2C-Cas9 RNPs were injected into adult females 1–2 months after adult emergence. (E) Eye color phenotypes of *cardinal* mutants. Eyes were photographed on the day of adult emergence (adult day 0). (F) Sanger electropherogram of the genomic PCR product of a white-eyed G_1 mutant male. Note the presence of a 4 bp deletion in this G_1 male, which introduces a premature stop codon indicated by a blue box and the absence of the trace of other alleles. PAM,

protospacer adjacent motif. (G) Nucleotide sequence of the cd^{ReMOT} allele. The cd^{ReMOT} allele (bottom) has a 4 bp deletion located upstream of the PAM. The nucleotide sequence targeted by sgRNA1 is underlined.

Fig. 2.6. Nucleotide and amino acid sequence of *cd*^{ReMOT} allele

(A) Alignment of the nucleotide sequences of *cardinal* around the sgRNA1 target site (exon 3). Note the presence of a 4-bp deletion in the *cd*^{ReMOT} allele (shown in orange). The premature stop codon induced by this deletion is shown in blue. (B) Alignment of the amino acid sequences of *cardinal* of the *wt* and *cd*^{ReMOT} strains. The 4 bp deletion shown in (A) caused a frameshift mutation in the *cd*^{ReMOT} allele (shown in orange letters).

Purpose	Parental cross (female × male)	White eyes		Black eyes	
		Female	Male	Female	Male
Inheritance mode	+/+ × cd^{ReMOT}/Y[a]	0	0	>50	>50
	cd^{ReMOT}/+ × +/Y	0	86	174	91
Complementation test	cd^{ReMOT}/cd^{ReMOT} × *red-1*/Y	78	114	0	0
	cd^{ReMOT}/cd^{ReMOT} × *peach*/Y	115	97	0	0

a, G_1 male

Table 2.2. Results of crossing experiments

The *cardinal* gene is responsible for the *red-1* and *peach* mutations

I performed complementation tests between cd^{ReMOT} and the *red-1* or *peach* alleles. As shown in Table 2.2, all of the F_1 adults obtained from the crosses of cd^{ReMOT} females × *red-1* or *peach* males had white eyes. In addition, all of the F_1 adults from the reciprocal crosses also had white eyes, suggesting that the white eye phenotype of the *red-1* or *peach* alleles was not complemented by the cd^{ReMOT} allele. These results provide definitive evidence that *cardinal* is responsible for the *red-1* and *peach* mutations.

2.4 Discussion

It has been shown that *cardinal* mutant adults of *Drosophila* and *Bombyx* have altered eye colors, and accumulate the ommochrome precursor 3-hydroxykynurenine (Harris et al., 2011; Osanai-Futahashi et al., 2016). In *Drosophila*, the eye color of newly-emerged *cardinal* mutants becomes close to the normal eye color of the wild type during aging. I found a similar phenotype in *Tribolium cardinal* mutants: the eyes are white at the time of eclosion, but gradually turn red in both spontaneous (*red-1* and *peach*) and CRISPR/Cas9-induced mutants (cd^{ReMOT}) (data not shown). One explanation for this color change could be the auto-oxidation of 3-hydroxykynurenine into reddish-brown xanthommatin (Osanai-Futahashi et al., 2016; Zhang et al., 2017). Although ommochromes are the major pigments in the eyes of most insects, they are also present as pigments in other tissues, such as wings and larval epidermis. For example, ommochrome pigments are known to be present in the wings of some butterflies such as *Heliconius* and *Precis* (Gilbert et al., 1998), and in some larval body markings in *Bombyx* (Osanai-Futahashi et al., 2016). However, I did not observe any apparently abnormal coloration other than that of the eyes in *Tribolium cardinal* mutants. The role of *cardinal* in

ommochrome biosynthesis is evolutionally conserved over numerous taxa of insects, including *Tribolium*, *Drosophila*, *Bombyx*, and the brown planthopper *Nilaparvata lugens* (Liu et al., 2019), suggesting that gene regulation of *cardinal* has become greatly diversified, depending on insect color patterns. I hope that the present study will encourage future studies into the function and diversification of the ommochrome biosynthetic genes in insects.

The present study has another important outcome: I here describe the first successful example of ReMOT Control-mediated targeted gene disruption (Chaverra-Rodriguez et al., 2018) in a beetle. CRISPR/Cas system has been widely used in many organisms, including animals and plants (Doudna and Charpentier, 2014). In insects, however, the requirement for injection into early embryos greatly limits the applicability of this system to diverse insect species. For instance, some species have very hard chorions that hamper embryo injection; the eggs of some species are encased by the oothecae or densely covered with glue; and some species produce nymphs or larvae instead of eggs. In addition, conventional embryo injection requires a specific experimental setup for each species, involves time-consuming training of researchers with regard to injection skills, and must be completed in a small time window, from oviposition to the preblastoderm stage. As Cas9 RNP can be delivered into vitellogenic oocytes in injected female adults, ReMOT Control should be able to circumvent these problems, as it simply requires adult injection (Chaverra-Rodriguez et al., 2018).

My results indicate that *cardinal* is an excellent target with which to develop a practical method for maternal gene disruption in *Tribolium*, for the following two reasons: (1) *cardinal* mutants can be screened in progeny males (G_1) of injected females (G_0) without molecular diagnosis; and (2) null mutants of *cardinal* are viable and fertile. Therefore, my results strongly suggest that a similar approach is promising in other insects, and probably also in other arthropods and vertebrates in which males are heterogametic (XY or XO).

In the original report of ReMOT Control, Cas9 was fused with a fragment of

Drosophila yolk protein 1, the P2C ligand, and it was shown that P2C-Cas9 RNP injected into females of the mosquito *Aedes aegypti* was able to induce efficient targeted mutagenesis in oocytes (Chaverra-Rodriguez et al., 2018). It has recently been shown that ReMOT Control works efficiently in another mosquito species, *Anopheles stephensi* (Macias et al., 2020). Although I have shown that ReMOT Control-mediated targeted mutagenesis can be achieved in *Tribolium*, the efficiency of the approach in this species appeared to be much lower than that reported in mosquitoes (Chaverra-Rodriguez et al., 2018; Macias et al., 2020). I speculate that this difference may be explained by differences in activity of the P2C ligand in mosquitoes and *Tribolium*. The P2C ligand is derived from *Drosophila*, which belongs to the same order, Diptera, as mosquitoes, and this ligand may therefore act efficiently in mosquitoes but not in *Tribolium*, which belongs to the order Coleoptera. In addition, experimental conditions, such as the concentration of Cas9 RNP and the type of endosomal escape reagent, which facilitates the release of Cas9 RNP from the endosome (Chaverra-Rodriguez et al., 2018; Macias et al., 2020), may need to be optimized for beetles.

Nevertheless, my successful example of ReMOT Control in *Tribolium* is encouraging for the future development of more efficient and versatile systems for insect genome editing via simple, low-cost adult injection. One promising approach will be the development of a novel tag that is specifically tuned to a target species. It would also be valuable to develop a ligand that has a broad host range and high efficiency. One candidate for the latter approach would be the use of vitellogenin, a precursor of vitellin, because vitellogenin is widespread in insects (Raikhel and Dhadialla, 1992; Sappington et al., 1998). As orthologs of the *Drosophila yolk protein*, from which P2C was derived, are present only in higher dipterans(Sappington, 2002), P2C may not work efficiently in non-dipteran insects. To test this idea, I am currently developing a novel vitellogenin-based tag for ovary transduction of Cas9 RNP in diverse insect species.

It is also noteworthy that vitellogenin is widely conserved in arthropods and oviparous vertebrates including fish, amphibians, reptiles, and birds (Polzonetti-Magni et al., 2004; Robinson, 2008; Romano et al., 2004). Importantly, a similar approach has been undertaken in medaka fish, and it was shown that a 300-aa fragment of medaka vitellogenin, which contains the secretory signal peptide and a putative receptor-binding region (Li et al., 2003), could work as a signal sequence for ovary transduction of GFP when the fusion protein was expressed in the liver by a transgene (Murakami et al., 2019). Given the widespread distribution of vitellogenin, a vitellogenin-based tag would become an important tool for ovary transduction of cargo proteins in a wide variety of animals.

2.5. References

Berghammer, A.J., Weber, M., Trauner, J., Klingler, M., 2009. Red flour beetle (*Tribolium*) germline transformation and insertional mutagenesis. Cold Spring Harb. Protoc. 4, 1–7. https://doi.org/10.1101/pdb.prot5259

Brown, S.J., Shippy, T.D., Miller, S., Bolognesi, R., Beeman, R.W., Lorenzen, M.D., Bucher, G., Wimmer, E.A., Klingler, M., 2009. The red flour beetle, *Tribolium castaneum* (Coleoptera): A model for studies of development and pest biology. Cold Spring Harb. Protoc. 4, 1–10. https://doi.org/10.1101/pdb.emo126

Chaverra-Rodriguez, D., Macias, V.M., Hughes, G.L., Pujhari, S., Suzuki, Y., Peterson, D.R., Kim, D., McKeand, S., Rasgon, J.L., 2018. Targeted delivery of CRISPR-Cas9 ribonucleoprotein into arthropod ovaries for heritable germline gene editing. Nat. Commun. 9, 1–11. https://doi.org/10.1038/s41467-018-05425-9

Daimon, T., Uchibori, M., Nakao, H., Sezutsu, H., Shinoda, T., 2015. Knockout silkworms

reveal a dispensable role for juvenile hormones in holometabolous life cycle. Proc. Natl. Acad. Sci. 112, E4226–E4235. https://doi.org/10.1073/pnas.1506645112

Doudna, J.A., Charpentier, E., 2014. The new frontier of genome engineering with CRISPR-Cas9. Science 346, 6213, 1258096. https://doi.org/10.1126/science.1258096

Eddleman, H., Bell, A., 1963. 4 new eye color mutants in *Tribolium castaneum*. Genetics 888.

Figon, F., Casas, J., 2019. Ommochromes in invertebrates: biochemistry and cell biology. Biol. Rev. 94, 156–183. https://doi.org/10.1111/brv.12441

Gilbert, L.I., Serafin, R.B., Watkins, N.L., Richard, D.S., 1998. Ecdysteroids regulate yolk protein uptake by *Drosophila melanogaster* oocytes. J. Insect Physiol. 44, 637–644.

Harris, D.A., Kim, K., Nakahara, K., Vásquez-Doorman, C., Carthew, R.W., 2011. Cargo sorting to lysosome-related organelles regulates siRNA-mediated gene silencing. J. Cell Biol. 194, 77–87. https://doi.org/10.1083/jcb.201102021

Hwang, W.Y., Fu, Y., Reyon, D., Maeder, M.L., Tsai, S.Q., Sander, J.D., Peterson, R.T., Yeh, J.R.J., Joung, J.K., 2013. Efficient genome editing in zebrafish using a CRISPR-Cas system. Nat. Biotechnol. 31, 227–229. https://doi.org/10.1038/nbt.2501

Lasley, E.L., 1960. Section new mutants. Tribolium Inf. Bull 3, 17.

Li, A., Sadasivam, M., Ding, J.L., 2003. Receptor-ligand interaction between vitellogenin receptor (VtgR) and vitellogenin (Vtg), implications on low density lipoprotein receptor and apolipoprotein B/E. J. Biol. Chem. 278, 2799–2806. https://doi.org/10.1074/jbc.m205067200

Liang, Z., Chen, K., Li, T., Zhang, Y., Wang, Y., Zhao, Q., Liu, J., Zhang, H., Liu, C., Ran, Y., Gao, C., 2017. Efficient DNA-free genome editing of bread wheat using CRISPR/Cas9 ribonucleoprotein complexes. Nat. Commun. 8, 6–10. https://doi.org/10.1038/ncomms14261

Liu, S.H., Luo, J., Yang, B.J., Wang, A.Y., Tang, J., 2019. *karmoisin* and *cardinal* ortholog

genes participate in the ommochrome synthesis of *Nilaparvata lugens* (Hemiptera: Delphacidae). Insect Sci. 26, 35–43. https://doi.org/10.1111/1744-7917.12501

Lorenzen, M.D., Brown, S.J., Denell, R.E., Beeman, R.W., 2002. Cloning and characterization of the *Tribolium castaneum* eye-color genes encoding tryptophan oxygenase and kynurenine 3-monooxygenase. Genetics 160, 225–234. https://doi.org/10.1093/genetics/160.1.225

Macias, V.M., McKeand, S., Chaverra-Rodriguez, D., Hughes, G.L., Fazekas, A., Pujhari, S., Jasinskiene, N., James, A.A., Rasgon, J.L., 2020. Cas9-mediated gene-editing in the malaria mosquito *Anopheles stephensi* by ReMOT Control. G3 Genes, Genomes, Genet. 10, 1353–1360. https://doi.org/10.1534/g3.120.401133

Murakami, Y., Horibe, T., Kinoshita, M., 2019. Development of an efficient bioreactor system for delivering foreign proteins secreted from liver into eggs with a vitellogenin signal in medaka *Oryzias latipes*. Fish. Sci. 85, 677–685. https://doi.org/10.1007/s12562-019-01320-4

Naito, Y., Hino, K., Bono, H., Ui-Tei, K., 2015. CRISPRdirect: Software for designing CRISPR/Cas guide RNA with reduced off-target sites. Bioinformatics 31, 1120–1123. https://doi.org/10.1093/bioinformatics/btu743

Osanai-Futahashi, M., Tatematsu, K.I., Futahashi, R., Narukawa, J., Takasu, Y., Kayukawa, T., Shinoda, T., Ishige, T., Yajima, S., Tamura, T., Yamamoto, K., Sezutsu, H., 2016. Positional cloning of a *Bombyx* pink-eyed white egg locus reveals the major role of cardinal in ommochrome synthesis. Heredity 116, 135–145. https://doi.org/10.1038/hdy.2015.74

Polzonetti-Magni, A.M., Mosconi, G., Soverchia, L., Kikuyama, S., Carnevali, O., 2004. Multihormonal control of vitellogenesis in lower vertebrates. Int. Rev. Cytol 239, 1–46

Raikhel, A.S., Dhadialla, T.S., 1992. Accumulation of yolk proteins in insect oocytes. Annu.

Rev. Entomol. 37, 217–251. https://doi.org/10.1146/annurev.ento.37.1.217

Richards, S., Gibbs, R.A., Weinstock, G.M., Brown, S., Denell, R., Beeman, R.W., Gibbs, R., Bucher, G., Friedrich, M., Grimmelikhuijzen, C.J.P., Klingler, M., Lorenzen, M., Roth, S., Schröder, R., Tautz, D., Zdobnov, E.M., Muzny, D., Attaway, T., Bell, S., Buhay, C.J., Chandrabose, M.N., Chavez, D., Clerk-Blankenburg, K.P., Cree, A., Dao, M., Davis, C., Chacko, J., Dinh, H., Dugan-Rocha, S., Fowler, G., Garner, T.T., Garnes, J., Gnirke, A., Hawes, A., Hernandez, J., Hines, S., Holder, M., Hume, J., Jhangiani, S.N., Joshi, V., Khan, Z.M., Jackson, L., Kovar, C., Kowis, A., Lee, S., Lewis, L.R., Margolis, J., Morgan, M., Nazareth, L. V., Nguyen, N., Okwuonu, G., Parker, D., Ruiz, S.J., Santibanez, J., Savard, J., Scherer, S.E., Schneider, B., Sodergren, E., Vattahil, S., Villasana, D., White, C.S., Wright, R., Park, Y., Lord, J., Oppert, B., Wang, L., Weinstock, G., Liu, Y., Worley, K., Elsik, C.G., Reese, J.T., Elhaik, E., Landan, G., Graur, D., Arensburger, P., Atkinson, P., Beidler, J., Demuth, J.P., Drury, D.W., Du, Y.Z., Fujiwara, H., Maselli, V., Osanai, M., Robertson, H.M., Tu, Z., Wang, J.J., Wang, S., Song, H., Zhang, L., Werner, D., Stanke, M., Morgenstern, B., Solovyev, V., Kosarev, P., Brown, G., Chen, H.C., Ermolaeva, O., Hlavina, W., Kapustin, Y., Kiryutin, B., Kitts, P., Maglott, D., Pruitt, K., Sapojnikov, V., Souvorov, A., Mackey, A.J., Waterhouse, R.M., Wyder, S., Kriventseva, E. V., Kadowaki, T., Bork, P., Aranda, M., Bao, R., Beermann, A., Berns, N., Bolognesi, R., Bonneton, F., Bopp, D., Butts, T., Chaumot, A., Denell, R.E., Ferrier, D.E.K., Gordon, C.M., Jindra, M., Lan, Q., Lattorff, H.M.G., Laudet, V., Von Levetsow, C., Liu, Z., Lutz, R., Lynch, J.A., Da Fonseca, R.N., Posnien, N., Reuter, R., Schinko, J.B., Schmitt, C., Schoppmeier, M., Shippy, T.D., Simonnet, F., Marques-Souza, H., Tomoyasu, Y., Trauner, J., Van Der Zee, M., Vervoort, M., Wittkopp, N., Wimmer, E.A., Yang, X., Jones, A.K., Sattelle, D.B., Ebert, P.R., Nelson, D., Scott, J.G., Muthukrishnan, S., Kramer, K.J., Arakane, Y., Zhu, Q., Hogenkamp, D., Dixit, R., Jiang, H., Zou, Z., Lu,

Z., Zhao, P., Sumathipala, N., Elpidina, E., Vinokurov, K., Evans, J., Altincicek, B., Vilcinskas, A., Williams, M., Hultmark, D., Hetru, C., Hauser, F., Cazzamali, G., Williamson, M., Li, B., Tanaka, Y., Predel, R., Neupert, S., Schachtner, J., Verleyen, P., Raible, F., Walden, K.K.O., Angeli, S., Forêt, S., Schuetz, S., Maleszka, R., Miller, S.C., Grossmann, D., 2008. The genome of the model beetle and pest *Tribolium castaneum*. Nature 452, 949–955. https://doi.org/10.1038/nature06784

Robinson, R., 2008. For mammals, loss of yolk and gain of milk went hand in hand. PLoS Biol. 6, 0421. https://doi.org/10.1371/journal.pbio.0060077

Romano, M., Rosanova, P., Anteo, C., Limatola, E., 2004. Vertebrate yolk proteins: A review. Mol. Reprod. Dev. 69, 109–116. https://doi.org/10.1002/mrd.20146

Sappington, T.W., 2002. The major yolk proteins of higher diptera are homologs of a class of minor yolk proteins in lepidoptera. J. Mol. Evol. 55, 470–475. https://doi.org/10.1007/s00239-002-2342-0

Sappington, T.W., Sappington, T.W., Raikhel, A.S., 1998. Molecular characteristics of insect vitellogenins and vitellogenin receptors molecular characteristics of insect vitellogenins and vitellogenin receptors. Insect Biochem. Mol. Biol. 28, 277–300. https://doi.org/10.1016/S0965-1748(97)00110-0

Searles, L.L., Ruth, R.S., Pret, A.M., Fridell, R.A., Ali, A.J., 1990. Structure and transcription of the *Drosophila melanogaster vermilion* gene and several mutant alleles. Mol. Cell. Biol. 10, 1423–1431. https://doi.org/10.1128/mcb.10.4.1423

Searles, L.L., Voelker, R.A., 1986. Molecular characterization of the *Drosophila vermilion* locus and its suppressible alleles. Proc. Natl. Acad. Sci. U. S. A. 83, 404–408. https://doi.org/10.1073/pnas.83.2.404

Tatematsu, K. ichiro, Yamamoto, K., Uchino, K., Narukawa, J., Iizuka, T., Banno, Y., Katsuma, S., Shimada, T., Tamura, T., Sezutsu, H., Daimon, T., 2011. Positional cloning

of silkworm *white egg 2* (*w-2*) locus shows functional conservation and diversification of ABC transporters for pigmentation in insects. Genes to Cells 16, 331–342. https://doi.org/10.1111/j.1365-2443.2011.01490.x

Warren, W.D., 1996. Molecular characterization of the cinnabar region of *Drosophila melanogaster*: Identification of the *cinnabar* transcription unit. Genetica 98, 249–262. https://doi.org/10.1007/BF00057589

Yamada, Y., 1961. Section on new mutants. Tribolium Inf. Bull 5, 13.

Zhang, H., Lin, Y., Shen, G., Tan, X., Lei, C., Long, W., Liu, H., Zhang, Y., Xu, Y., Wu, J., Gu, J., Xia, Q., Zhao, P., 2017. Pigmentary analysis of eggs of the silkworm *Bombyx mori*. J. Insect Physiol. 101, 142–150. https://doi.org/10.1016/j.jinsphys.2017.07.013

Chapter 3
Development of the DIPA-CRISPR method

3.1 Introduction

Recent advances in genome editing tools have enabled sophisticated engineering of insect genomes (Doudna and Charpentier, 2014; Gantz and Akbari, 2018; Matthews and Vosshall, 2020). However, current approaches rely on embryo injection, which require expensive equipment, a specific experimental setup for each species, and highly skilled laboratory personnel (Matthews and Vosshall, 2020; Tamura et al., 2000). Furthermore, embryo injection must be completed in a small time window, from oviposition to preblastoderm stage, which is not applicable to species that give live birth rather than lay eggs (e.g., viviparous aphids and flies) or species in which an access to very early embryos is highly challenging (e.g., cockroaches, which encapsulate the eggs into a hard egg case or ootheca).

Recently, an alternative method that can bypass the requirement of embryo injection has been developed in the mosquito *Aedes aegypti* (Chaverra-Rodriguez et al., 2018). In this method, called Receptor-Mediated Ovary Transduction of Cargo (ReMOT), peptide ligands derived from yolk protein precursors are fused to Cas9 protein, and the complex of the engineered Cas9 and single-guide RNAs (sgRNAs) is injected into female adults to introduce mutations in developing oocytes. ReMOT-mediated targeted mutagenesis has been successfully used in a few other species, such as the mosquito *Anopheles stephensi* (Macias et al., 2020), the jewel wasp *Nasonia vitripennis* (Chaverra-Rodriguez et al., 2020), the red flour beetle *Tribolium castaneum* (Shirai and Daimon, 2020), and the silverleaf whitefly *Bemisia*

tabaci (Heu et al., 2020). Although these examples are encouraging, the ReMOT approach appears to have a number of limitations. For example, the results reported so far indicate that the peptide ligands that are fused to Cas9 should be specifically tuned to a target species for efficient genome editing (Chaverra-Rodriguez et al., 2018; Heu et al., 2020; Shirai and Daimon, 2020), which may be a barrier for non-specialist laboratories.

Interestingly, however, the above studies, together with the study in the spider mite *Tetranychus urticae* (Dermauw et al., 2020), also showed that a very small number of gene-edited individuals could be recovered by adult injection of non-tagged Cas9 (i.e., Cas9 without a ligand sequence). Thus, these studies suggest that, although the addition of an appropriate ligand tag to Cas9 could increase genome editing efficiency, its addition is not essential for genome editing by adult injection.

During the course of my work aiming at developing a novel peptide tag for Cas9 that can cover a broad range of insect groups by a single ligand sequence (i.e., a fragment of yolk protein precursor vitellogenin (Li et al., 2003; Murakami et al., 2019; discussed in Shirai and Daimon, 2020), I found that female adult injection of non-tagged Cas9 can efficiently introduce heritable mutations in developing oocytes of the German cockroach *Blattella germanica*, to which conventional approaches (i.e., embryo injection) are not feasible. As I used commercially available standard Cas9 protein (i.e., the one sold for general genome editing experiments in animals and cultured cells), such 'non-tagged Cas9 approach' would become a more generalized method for insect genome editing by adult injection. To further explore this possibility, I here optimized this method and established it as an accessible technology for insect genome editing, which I named "direct parental" CRISPR (DIPA-CRISPR).

After exploring different optimizing conditions of DIPA-CRISPR in *B. germanica*, I demonstrated that genome editing efficiency (GEF; the proportion of edited individuals out of

the total number of individuals hatched) could reach as high as 21.8%, which easily enabled the first establishment of knockout cockroach lines. Furthermore, I tested DIPA-CRISPR in the red flour beetle *T. castaneum*, in which GEF reached over 50%, a percentage comparable with the efficiency reached in conventional approaches (Gilles et al., 2015). Furthermore, I was able to generate gene knock-in beetles by co-injecting single-stranded oligonucleotides (ssODNs) and Cas9 RNPs. The successful application of DIPA-CRISPR in the two evolutionarily distant insect species gives an idea of its generalizability. Without the need of custom-engineering of Cas9 or the use of special reagents that have been considered to facilitate the ovary uptake of injected Cas9 ribonucleoproteins (RNPs) (Chaverra-Rodriguez et al., 2018; Chaverra‐Rodriguez et al., 2020), DIPA-CRISPR could be readily implemented in any laboratory, so that it would greatly extend the application of genome editing to a wide diversity of insect species.

3.2 Materials and Methods

Insects

A *Blattella germanica* colony derived from a Japanese population was maintained at 25 ± 1.5°C under a 16 h:8 h light:dark cycle with a constant supply of solid feed (MF, Oriental Yeast) and water. A *Tribolium castaneum* (Okinawa strain) colony was maintained on wheat flour containing 5% (w/w) brewer's dry yeast at 30 ± 1°C and 50%–70% relative humidity as described previously (Shirai and Daimon, 2020). The wildtype *Drosophila melanogaster* strain (Canton S) was reared using a commercial Drosophila diet (Formula 4-24 Instant Drosophila Food, Carolina Biological).

Preparation of Cas9-sgRNA RNPs

Single-guide RNAs (sgRNAs) targeting *B. germanica cinnabar* (PSN36199), *T. castaneum cardinal* (XP_008200769), and *D. melanogaster white* (NM_057439) were synthesized as described previously (Shirai and Daimon, 2020). Briefly, annealed oligo DNA was cloned into the BsaI site of the pDR274 vector (Hwang et al., 2013). After linearization with DraI, the vector was used as a template for *in vitro* transcription using the T7 RiboMAX Express Large Scale RNA Production System (Promega). The synthesized sgRNAs were extracted with phenol (pH4–5):chloroform:isoamyl alcohol (125:24:1) (Sigma), and then precipitated with isopropanol and dissolved in RNase-free water. For *D. melanogaster white*, I also purchased and used chemically synthesized sgRNAs from the Integrated DNA Technologies (IDT) (Alt-R® CRISPR-Cas9 sgRNA). Otherwise stated, commercial Cas9 protein purchased from IDT (Alt-R® S.p. Cas9 Nuclease V3), which has nuclear localization signals and a C-terminal 6-His tag (further details were not disclosed to the authors), was used in this study. Cas9 protein and sgRNAs were mixed at a molar ratio of approximately 1:2, and incubated for 10–15 min at room temperature to allow Cas9 RNP formation. In some experiments, freshly-prepared chloroquine (FUJIFILM Wako) or saponin (Sigma) was added as an endosomal escape reagent (EER) (Chaverra-Rodriguez et al., 2018). Concentrations of Cas9 RNPs and EERs in the injection solution were adjusted with RNase-free water, without adding any other reagents (e.g., buffers or salts). The target sequences of sgRNAs are (5'- to -3'): GGTCTGGCTGTAGTCAAACA for *B. germanica cinnabar* sgRNA1; TTGGAGGCATGCAAAGCTCC for *B. germanica cinnabar* sgRNA2; GGAACAGATGAACCAAGTGA for *T. castaneum cardinal* sgRNA1 (Shirai and Daimon, 2020); CATTAACCAGGGCTTCGGGC for *D. melanogaster white* sgRNA1 (Ren et al., 2014); and AGCGACACATACCGGCGCCC for *D. melanogaster white* sgRNA2 (Ren et al., 2014).

Adult injection and mutant screening in *Blattella germanica*

Female adults carrying the ootheca were collected from a stock colony, monitored daily for ootheca drop, and were staged based on the day after the ootheca drop. The injection was performed using a glass capillary needle equipped with Femtojet 4i (Eppendorf). The females used for injection were anesthetized on ice. Approximately 4 µl of the Cas9 RNP solution containing 3.3 µg/µl Cas9 (IDT) and 1.3 µg/µl sgRNAs (a mixture of sgRNA1 and sgRNA2, Figure 3.2A) with or without chloroquine (2 mM) was injected into the ventral abdomen of the female adults. Injected females were individually reared in containers until the formation of the next ootheca and hatching of G_0 nymphs (nymphs hatched ~20–30 days after injection with ~20–50 nymphs hatched from each ootheca). The eye colors of hatched G_0 nymphs were examined, and all the nymphs without external phenotypes were subjected to individual genotyping. *B. germanica cinnabar* is an autosomal gene, as I found heterozygous males [male = XO and female = XX in *B. germanica* (Meisel et al., 2019)].

Genotyping of *Blattella germanica*

Genomic DNAs were extracted individually as described previously (Daimon et al., 2015). Genomic PCR was conducted using KOD FX Neo (TOYOBO). Mutations were screened by analyzing the PCR products using the heteroduplex mobility assay (HMA) using the MultiNA Microchip Electrophoresis System (MCE-202, Shimadzu). Primer sequences for HMA of *B. germanica cinnabar* are (5'- to -3'): GAAGGCGGATTTGATCATAGGAGC and CAATCACTTACCTCACCATCTTCTG. To determine the nucleotide sequences of mutant alleles, Sanger sequencing chromatograms were analyzed with Poly Peak Parser program (Hill et al., 2014). Primer sequences for Sanger sequencing of *B. germanica cinnabar* are (5'- to -3'): GGCGCACTTGAGGCAGATATG and TTCCCCTACACTTCAATGCGGG.

Adult injection and mutant screening in *Tribolium castaneum*

Female adults at selected days after adult emergence, separated from males at the time of injection, were injected with approximately 0.5 μL of the Cas9 RNP solution containing 3.3 μg/μL Cas9 (IDT) and 1.3 μg/μL sgRNA, with or without saponin (100 ng/μL), as described previously (Shirai and Daimon, 2020). The injected females were grouped with males in a container with wheat flour and transferred to a new container every 24 hours to examine the relationship between the day of egg laying and the genome editing efficiencies in the hatchlings. To screen gene-edited individuals, the eye colors of the G_0 insects were examined during pupal and adult stages. I also examined and compared the performance of Cas9 products from three companies additional to IDT: Sigma (Cat #CAS9PROT), FUJIFILM Wako (Cat#316-08651), and Fasmac (Cat#GE-005-S), which have a single or multiple nuclear localization signals, by targeting cardinal under the same condition (i.e., the same stage of injection and concentration of reagents). As *cardinal* gene locates on the X chromosome (female = XX, male = XY) (Shirai and Daimon, 2020), mutant phenotypes are not visible in heterozygous females. As I screened G_0 insects based on phenotypes but not on genotypes, the GEF values for *T. castaneum cardinal* in this study were most likely underestimated. Primer sequences for Sanger sequencing of *T. castaneum cardinal* are (5'- to -3'): GGCCAAAACCGGGGCGCTTCC and CCGGAAGTTCGTGGGTACAAGCCCG (Shirai and Daimon, 2020).

Gene knock-in experiments in *Tribolium castaneum*

Female adults at optimized stages (i.e., 4–5 days after adult emergence) were injected as above. Injection solution contained 3.3 μg/μL Cas9 (IDT, Cat#1081059), 1.3 μg/μL sgRNA (sgRNA1 for *cardinal*), and ssODNs (1.6 μg/μL). ssODNs were purchased from IDT

(Ultramer DNA Oligonucleotides). Injected females were allowed to lay eggs for two days, and the recovered G_0 adults with both eyes whites were subjected to genotyping. For genotyping, genomic DNAs of G_0 adults were individually extracted, and used as a template for PCR. PCR products were digested with HindIII and analyzed by microchip electrophoresis using the MultiNA Microchip Electrophoresis System (MCE-202, Shimadzu). Primer sequences for *T. castaneum cardinal* are (5'- to -3'): GTCACACATCCGGAGTGCTTTCC and GAGTTCACCCCCTGACATCGTC. To determine the nucleotide sequences of knock-in alleles, PCR products were subcloned and subjected to Sanger sequencing.

Adult injection and mutant screening in *Drosophila melanogaster*

Female adults at selected times after adult emergence, separated from males at the time of injection, were injected with approximately 0.5 mL of the Cas9 RNP solution containing 3.3 μg/μL Cas9 (IDT, Cat#1081059) and 1.3 μg/μL sgRNA (a mixture of sgRNA1 and sgRNA2 for *white*), with or without chloroquine (0.5 or 2.0 mM). The injected females were grouped with males in a vial and transferred to a new vial every 24 hours. To screen gene-edited individuals, the eye colors of the G_0 insects were examined during adult stages.

3.3 Results and Discussion

Cockroach genome editing with DIPA-CRISPR

In general, cockroach females ovulate the oocytes into the genital atrium, where they are fertilized and then encapsulated into a hard egg case, or ootheca, where they will remain for days or weeks until egg hatching (Figure 3.1A) (Cornwell, 1968). Because of this unique

reproduction system, it is impracticable to inject materials into very early embryos, thus genetic manipulation of cockroaches (i.e., transgenesis or genome editing) has not been achieved so far. To investigate whether adult injection of Cas9 RNPs enables cockroach genome editing, I tested non-tagged Cas9 in *B. germanica*, a global urban pest whose genome has been sequenced (Harrison et al., 2018), by targeting the autosomal eye-color gene *cinnabar* (Figure 3.2), which is involved in the biosynthesis of ommochrome pigments (Lorenzen et al., 2002; Quan et al., 2002).

I first injected commercial Cas9 RNPs into 16 fully matured females not carrying oothecae (Figure 3.1B). I presumed that they were undergoing a vitellogenic cycle, thus the injected Cas9 RNPs might be non-selectively incorporated into the growing oocytes with vitellogenins by receptor-mediated endocytosis (Ciudad et al., 2006; Cooper and Hausman, 2007; Dermauw et al., 2020; Raikhel and Dhadialla, 1992). Notably, 31% (5 out of 16) of the injected females that produced an ootheca after the injection yielded gene-edited G_0 (generation zero) progeny. Of the nine edited G_0 nymphs recovered from 385 hatchlings (GEF = 2.3%), two were eye-color mosaics (Figure 3.1C), and the other seven carried edited alleles as judged by genotyping experiments (see Figure 3.1D for representative results). As *cinnabar* is an autosomal gene, the mosaic phenotypes observed in the G_0 insects indicate that the incorporated Cas9 RNPs might persist in the oocyte for several days (i.e., from injection to fertilization) and then disrupted paternal alleles after fertilization, yielding cells having biallelic mutations.

The results obtained in this first experiment encouraged me to explore optimal conditions of my method, DIPA-CRISPR, by using carefully staged adults. I tested females at selected days of their reproductive cycle (Cornwell, 1968; Pascual et al., 1992; Treiblmayr et al., 2006) and found that injecting 4 days after ootheca drop and eggs hatching resulted in the highest efficiency (Figures 3.1E and 3.2C). In this condition, all the seven injected females

produced gene-edited G_0 nymphs, and they yielded 57 edited nymphs from 262 hatchlings in total (GEF = 21.8%) (Figure 3.1E). Notably, some G_0 nymphs had “white” eyes (i.e., the entire surface of both eyes was white), suggesting that biallelic mutations were introduced at a very early stage of embryogenesis. When the GEF values of injected females were individually measured, some females had values exceeding 40% (Figure 3.2C). Collectively, my results show that highly efficient cockroach genome editing can be achieved by simple adult injection.

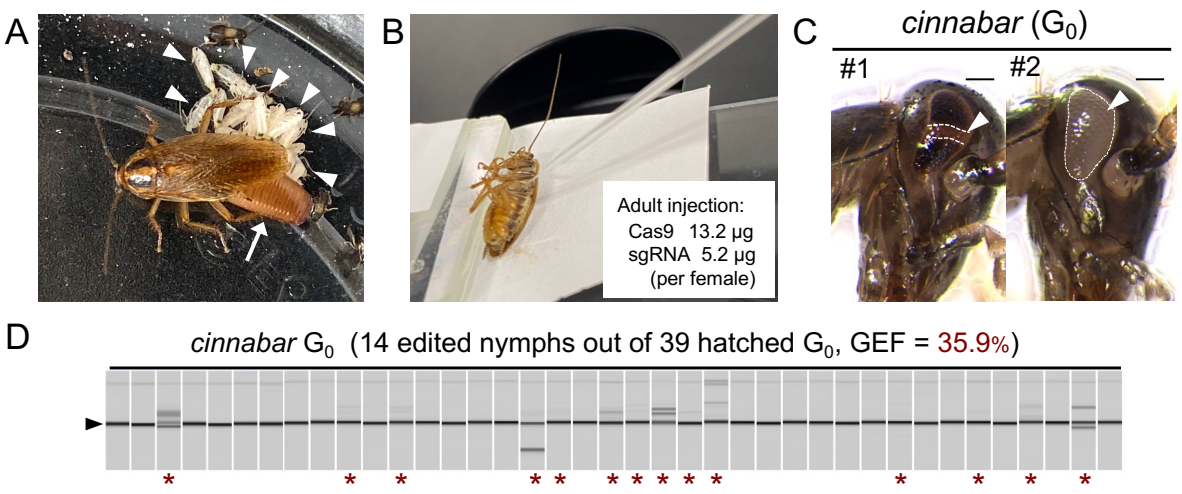

E

Gene	Stage of injection	EER	Females injected	Females survived/ laying G_0	Females laying G_0 mutants	Screened G_0	G_0 edited animals			Genome editing efficiency (GEF)
							white	mosaic	genotyping	
cinnabar	3 days AO	+	7	6	6 (100%)	226	1	1	21	10.2%
		-	10	8	4 (50.0%)	260			6	2.3%
	4 days AO	+	7	7	7 (100%)	262	3	7	47	21.8%
		-	9	7	5 (71.4%)	241	1	1	18	8.3%
	5 days AO	+	8	7	5 (71.4%)	215		2	23	11.6%
		-	7	6	6 (100%)	204	4	4	26	16.7%

Figure 3.1. Cockroach genome editing with DIPA-CRISPR

(A) Newly hatched nymphs (arrowheads) from the ootheca (arrow) of *Blattella germanica*. (B) Adult injection in *B. germanica*. (C) The eyes of cinnabar mosaic G_0 nymphs with loss of black eye pigments. Bars, 100 μm. (D) A representative result of cinnabar G_0 genotyping. G_0 nymphs with normal eyes hatched from a single ootheca were analyzed by heteroduplex mobility assay (HMA). Individuals having edited alleles (asterisks) and the homoduplex bands (156-bp, arrowhead) are indicated. See also Figure 2.2 for the detailed results. (E) Genome editing efficiency (GEF) of DIPA-CRISPR. G_0 mutants were first screened by phenotypes (white or mosaic), and then those without phenotypes were analyzed by HMA (genotyping). White, having phenotypes in entire regions

of both eyes; AO, after ootheca drop; EER, presence or absence of chloroquine (2 mM) in injection solution.

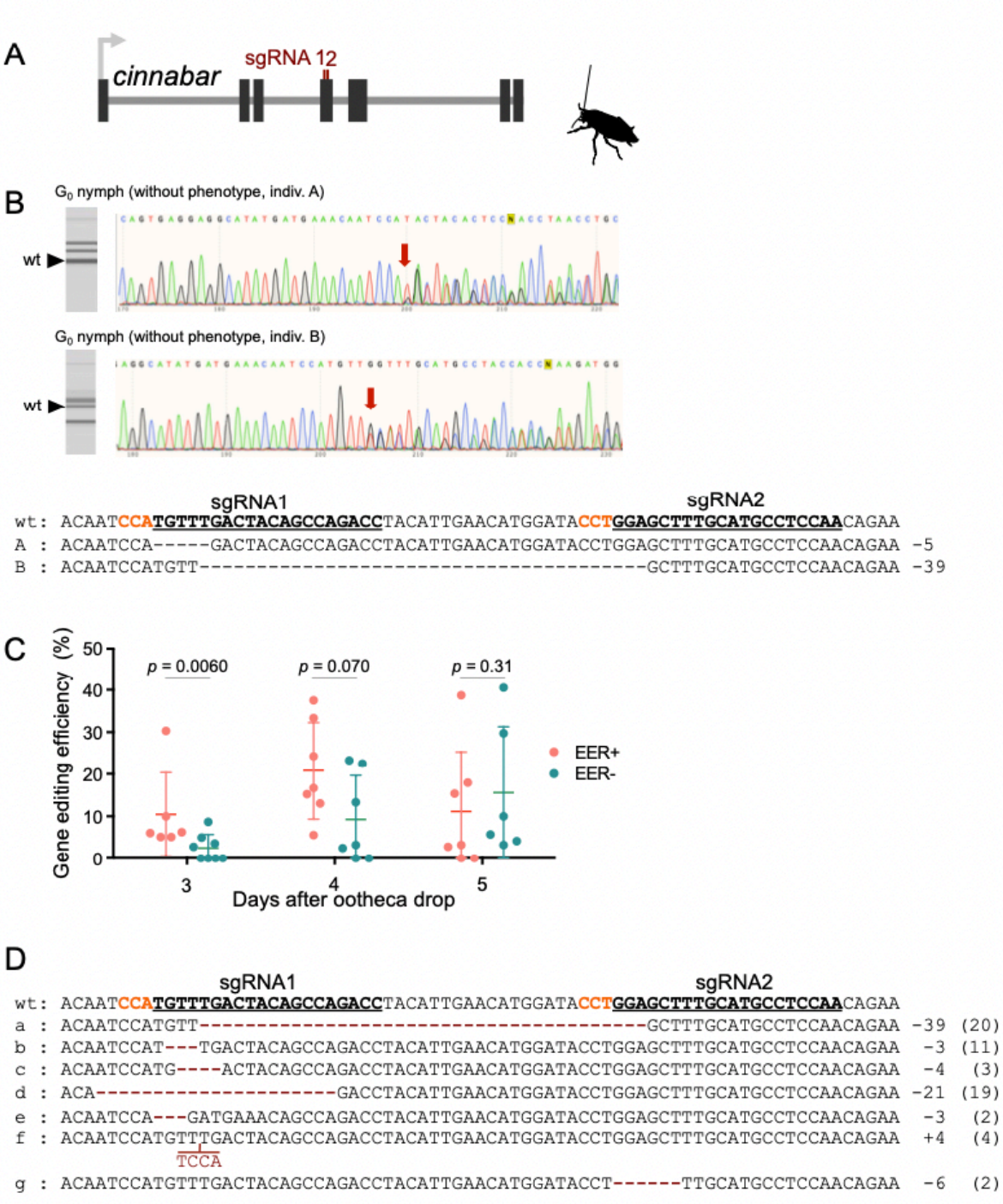

Figure 3.2. Disruption of *Blattella germanica cinnabar* by DIPA-CRISPR

(A) CRISPR target sites of *B. germanica cinnabar* (PSN36199). (B) Representative results of genotyping of G_0 edited nymphs. Two G_0 nymphs that carried mutations (judged by heteroduplex mobility assay) but do not show eye color phenotypes were subjected to direct Sanger sequencing of

genomic PCR products. Red arrows indicate the presence of double peaks caused by indel mutations. The DNA sequences of recovered mutant alleles are shown below the panel with sgRNA (underlined) and PAM (orange letters) sequences. (C) Genome editing efficiency (GEF) in the G_0 progenies. Each point represents an individual adult female injected. Bars indicate mean ± SD (n = 6–8). The GEF values were analyzed with the Mann-Whitney nonparametric U test. (D) The DNA sequences of *cinnabar* mutant alleles shown in Figure 3.2B (i.e., alleles a–g) with sgRNA (underlined) and PAM (orange letters) sequences. The length of indels and the number of G_1 insects (in parenthesis) are shown on the right.

Inheritance of edited alleles in cockroaches

To test if edited alleles in G_0 cockroaches are inherited to the next generation, I performed crossing experiments (Figure 3.3). When the two mosaic nymphs obtained in the first experiment (Figure 3.1C) were reared to adults and crossed to wild type (Figure 3.3A), 62.2% and 75.0% of their respective progenies (G_1) were heterozygous mutants (Figure 3.3B), showing very high germline mutation rates in these mosaics. To further confirm this result, G_0 adults with eye-color phenotypes (white or mosaic) were crossed and their G_1 progenies were screened for knockout phenotypes (Figure 3.3C). Notably, when G_0 adults with both eyes white were crossed, all of their G_1 progeny became white-eyed knockout insects (Figure 3.3D and E). This suggests that *cinnabar* was disrupted in all (or practically all) cells in the white-eyed G_0 individuals. Similarly, very high germline mutation rates were also exhibited in mosaic-eyed G_0 adults, which were roughly estimated to be > 50% (Figure 3.3E). Together, my results demonstrate that DIPA-CRISPR is a powerful method that easily enabled the first establishment of knockout cockroaches.

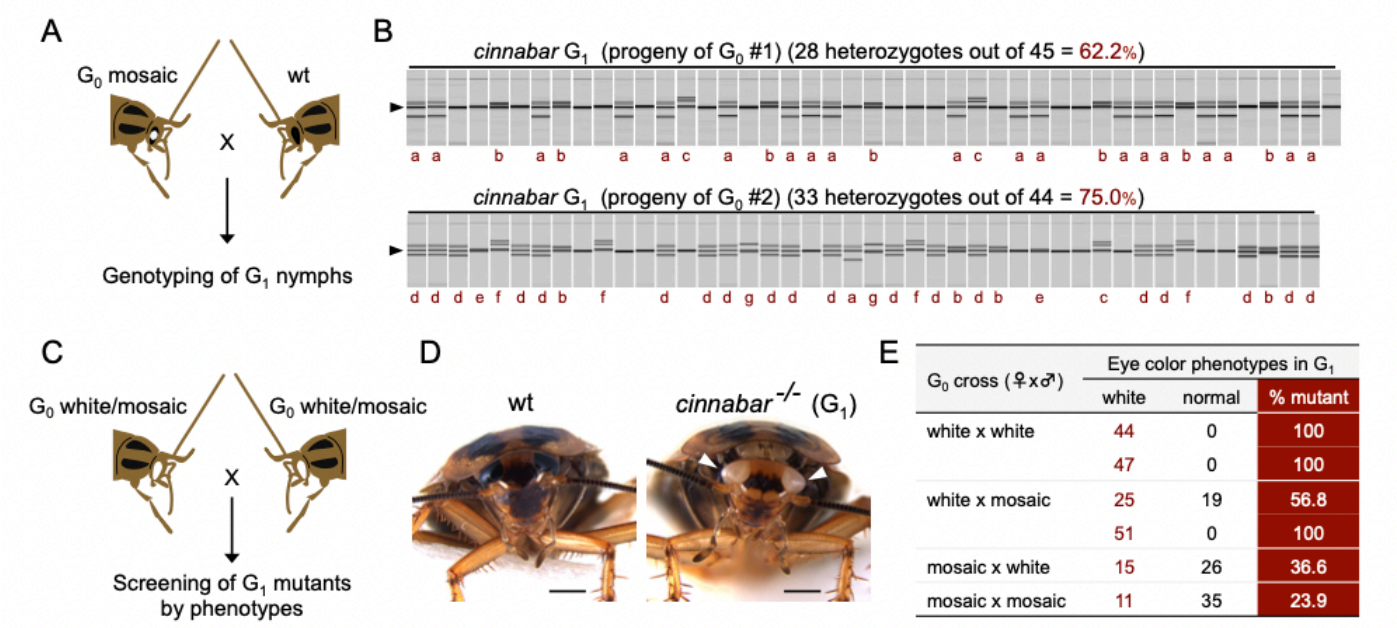

E

G0 cross (♀x♂)	Eye color phenotypes in G1		
	white	normal	% mutant
white x white	44	0	100
	47	0	100
white x mosaic	25	19	56.8
	51	0	100
mosaic x white	15	26	36.6
mosaic x mosaic	11	35	23.9

Figure 3.3. Inheritance of edited alleles in cockroaches

(A and B) A mating scheme (A) and the results of genotyping (B) of G_1 individuals. The two cinnabar mosaics shown in Figure 1C (G_0 #1 and #2) were crossed to wildtype, and all the G_1 progeny were individually analyzed by heteroduplex mobility assay. The mutant alleles are indicated below the panels (a–g, seven alleles in total). See Figure 3.2D for their nucleotide sequences. (C) A mating scheme for screening of G_1 knockout insects. G_0 insects with eye-color phenotypes were crossed to obtain G_1 progenies. (D) A cinnabar knockout G_1 adult (right). Arrowheads indicate the white eyes. Bars, 1 mm. (E) Phenotypes in G_1 insects. Each row indicates the result of a single-pair mating of G_0.

DIPA-CRISPR in beetles

To demonstrate potential for broad use, I applied DIPA-CRISPR to much more evolutionarily modified species, the red flour beetle *T. castaneum* (Figure 3.4). For these experiments, I targeted *cardinal*, an eye-color gene on the X chromosome, as their mutant phenotypes are easily visible in hemizygous G_0 males without genotyping (females = XX and males = XY in *T. castaneum*) (Grubbs et al., 2015; Shirai and Daimon, 2020). I injected Cas9 RNPs into females at selected days after adult emergence (Figures 3.4A and 3.5). I found that injection into 4- or 5-day-old adult females exhibited very high genome editing efficiency, with the GEF values being as high as 50.8% for 4-day-old females (32 out of 63 hatchlings) and 71.4% for 5-day-old females (15 out of 21) (Figures 3.4B and 3.4C), which is comparable to the efficiency in conventional embryo injection approaches (Gilles et al., 2015).

Cockroaches and beetles used in this study are evolutionarily very distant (Polyneopteran vs. Endopterygote) (Harrison et al., 2018; Misof et al., 2014), show radically different modes of metamorphosis (hemimetabolan vs. holometabolan) (Belles, 2020), and have different types of ovaries (panoistic in *B. germanica* vs. telotrophic in *T. castaneum*) (Mclaughlin and Bratu, 2015). Further, previous ReMOT studies have shown that genome editing can be achieved by adult injection in wasps and mosquitos (Chaverra-Rodriguez et al., 2018; Chaverra‐Rodriguez et al., 2020; Macias et al., 2020), which have the most derived types of ovaries (i.e., polytrophic). Thus, these results point to DIPA-CRISPR as a generalizable approach for insect genome editing.

A

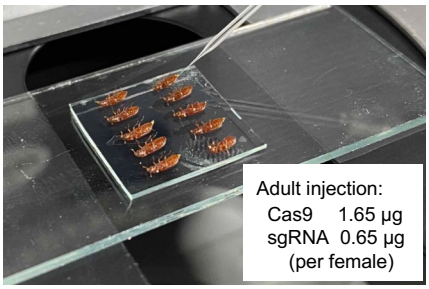

B

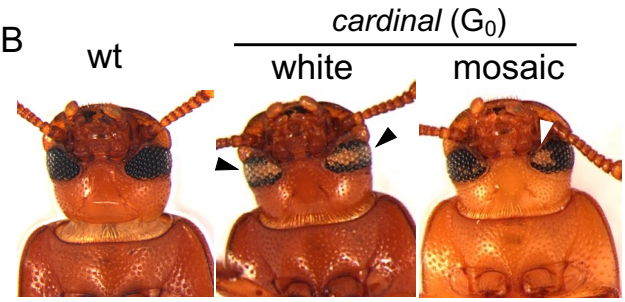

C

Gene	Stage of injection	EER	Females injected	Screened G_0	G_0 edited animals		Genome editing efficiency (GEF)
					white	mosaic	
cardinal	3 days AE	-	65	34			0%
		-	87	91			0%
	4 days AE	-	73	63	25	7	50.8%
		-	36	54	12	5	31.5%
	5 days AE	-	76	21	11	4	71.4%
		-	92	132	31	15	34.9%
	10 days AE	-	106	66	3	2	7.6%
		-	97	119	5	2	5.9%
	30 days AE	-	79	117	6	2	6.8%
		-	80	230	4	1	2.2%

D

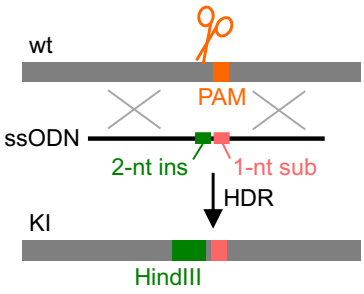

E

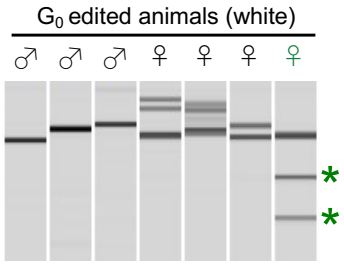

F

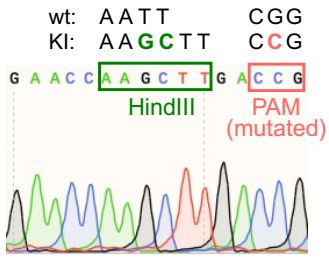

G

Gene	Stage of injection	EER	Females injected	G_0 white animals	G_0 knock-in animals	Knock-in efficiency
cardinal	4–5 days AE	-	289	39	1	2.6%
		-	364	151		
		-	164	55	2	3.6%

Figure 3.4. DIPA-CRISPR in beetles

(A) Adult injection in *Tribolium castaneum*. (B) G_0 adults generated by DIPA-CRISPR targeting *cardinal*. Arrowheads indicate the loss of black eye pigments. (C) The genome editing efficiency (GEF) in *T. castaneum*. See Figure 3.5 for the detailed results. (D) A scheme of knock-in using ssODNs as a template for homology-directed repair (HDR). ssODNs that contain 5′- and 3′-homology arms (96-nt each), a 2-nt nucleotide insertion (producing a HindIII site) and a 1-nt substitution (mutating the PAM sequence) are knocked into the cardinal gene. (E) A representative result of G_0 genotyping. G_0 adults with both eyes white were individually genotyped. The products of genomic PCR were digested with HindIII and analyzed by microchip electrophoresis. Asterisks indicate the HindIII-digested products. (F) The nucleotide sequence of the recovered knock-in (KI) allele. (G) The efficiency of knock-in through DIPA-CRISPR in three independent experiments. All the three knock-in beetles carried the precise knock-in allele shown in (F).

A

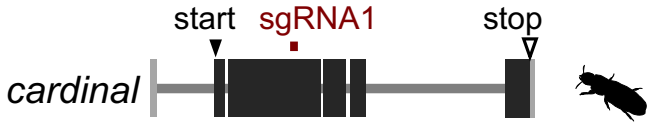

B

Gene	Stage of injection	EER	Females injected	Survival rates	Screened G_0	G_0 edited animals		Genome editing efficiency (GEF)
						white	mosaic	
cardinal	3 days AE	+	84	100%	85			0%
		+	68	100%	17			0%
		-	65	100%	34			0%
		-	87	98.9%	91			0%
	4 days AE	+	84	98.8%	9	5		55.6% [a]
		+	76	100%	4	1	2	75.0% [a]
		-	73	100%	63	25	7	50.8%
		-	36	97.2%	54	12	5	31.5%
	5 days AE	-	76	98.7%	21	11	4	71.4%
		-	92	100%	132	31	15	34.9%
	10 days AE	-	106	98.1%	66	3	2	7.6%
		-	97	99.0%	119	5	2	5.9%
	30 days AE	+	94	100%	133	3	2	3.8%
		+	88	97.7%	132			0%
		-	79	94.9%	117	6	2	6.8%
		-	80	97.5%	230	4	1	2.2%

C

sgRNA1

```
WT  1:GGCCCAGGGAACAGATGAACCAA----------GTGACGGCGTTTATAGACGG
#1  1:GGCCCAGGGAACAGATGAACCAA----------TGACGGCGTTTATAGACGG    -1
#4  1:GGCCCAGGGAACAGATGAACCAA----------GGCGTTTATAGACGG        -5
#5  1:GGCCCAGGGAACAGATGAACCAA----------GGCGTTTATAGACGG        -5
#6  1:GGCCCAGGGAACAGATGAACCAA----------GATGACGGCGTTTATAGACGG  +1
#7  1:GGCCCAGGGAACAGATGA----------CGGCGTTTATAGACGG            -9
#9  1:GGCCCAGGGAACAGATGAACCAA----------TGACGGCGTTTATAGACGG    -1
#20 1:GGCCCAGGGAACAGATGAACCAACA----------GATGACGGCGTTTATAGACGG  +3
#27 1:GGCCCAGGGAACAGATGAACCAAGAACAGGGAACAGATGACGGCGTTTATAGACGG  +13
#28 1:GGCCCAGGGAACAGATGA----------CGGCGTTTATAGACGG            -9
#29 1:GGCCCAGGGAACAGATGAACCACGGCGTTCATCGCGTTCACGGCGTTTATAGACGG  +13
#32 1:GGCCCAGGGAACAGATGAACAGA----------TGACGGCGTTTATAGACGG    -1
#34 1:GGCCCAGGGAACAGATGA----------CGGCGTTTATAGACGG            -9
#37 1:GGCCCAGGGAACAGATGA----------CGGCGTTTATAGACGG            -9
#42 1:GGCCCAGGGAACAGATGAACAGA----------TGACGGCGTTTATAGACGG    -1
#43 1:GGCCCAGGGAACAGATGAAC----------GTTTATAGACGG              -11
```

Figure 3.5. Disruption of *Tribolium castaneum cardinal* by DIPA-CRISPR

(A) The CRISPR target site of *T. castaneum cardinal* (XP_008200769). The sgRNA1 targeting the exon 3 of *cardinal* (Shirai and Daimon, 2020) was used. (B) The detailed results of DIPA-CRISPR in *T. castaneum*. Cas9 ribonucleoprotein (RNP) solution containing 3.3 μg/μL Cas9 (IDT) and 1.3 μg/μL sgRNA were injected into adult females of selected days (i.e., 3, 4, 5, 10 or 30 days) after adult emergence (AE). The injected females were pooled, and the results are from the eggs laid during the first 24 h (females at 4, 5, 10 or 30 days AE) or 48 h (females at 3 days AE, as they were too young to lay eggs during the first 24 h) after injection. The results from two independent experiments are shown. EER, presence (+) or absence (-) of an endosomal escape reagent saponin (100 ng/μL) in injection solution. a: the genome editing efficiency (GEF) values are very high, but these values may not be reliable as they are calculated based on very small numbers of G_0 insects hatched and/or survived. (C) The DNA sequences of *cardinal* mutant alleles in G_0 edited insects. Hemizygous G_0 males with white eyes were randomly chosen and subjected to direct Sanger sequencing of genomic PCR products. Each row represents each G_0 mutant, and the length of indel is shown on the right.

Gene knock-in by DIPA-CRISPR in beetles

I next tested whether DIPA-CRISPR could be used to generate gene knock-in insects, using *T. castaneum* as the experimental subject. I designed a ssODN having homology arms (96-nt each for 5′- and 3′-homology arms), a 2-nt insertion that introduces a novel HindIII restriction site, and a 1-nt substitution that mutates PAM, and used it as a template for homology-directed repair (HDR) (Figure 3.4D–G). After injecting a mixture of Cas9 RNPs targeting *cardinal* and the ssODNs into female adults at optimized stages, I screened for white-eyed G_0 adults. Genotyping of these adults showed that three adults (1.2%, 3 out of 245 in total) carried precise knock-in alleles generated by HDR (Figure 3.4E and F). Although the efficiency is still low and should be further improved, my results indicate that the application of DIPA-CRISPR can be extended to knock-in experiments.

Cas9 for DIPA-CRISPR

The direct use of commercial Cas9 protein for adult injection in the DIPA-CRISPR can eliminate time-consuming processes required in a similar adult injection approach (ReMOT) (Chaverra-Rodriguez et al., 2018), such as the development of a novel ligand that is tuned to target species, engineering of Cas9, and the expression and purification of recombinant Cas9 protein. Thus, the use of commercial Cas9 can enable genome editing in any non-specialist laboratory that cannot implement the above elaborated methods.

I also investigated and compared the performance of commercial Cas9 products from additional three companies in the market (Figure 3.6A). Although details were not disclosed to me, these Cas9 products should be engineered differently by manufacturers in many ways [e.g., the type, number, and location of nuclear localization signals (NLSs) or other epitope/purification tags]. Nevertheless, their genome editing efficiencies were comparable and very high when tested in *T. castaneum* (GEF = 24–32%, Figure 3.6A). This indicates that

there is little requirement to use a particular Cas9 product, although the presence of NLSs should be essential for the delivery of Cas9 RNPs to the nucleus.

It is of note that, unlike this study, very little genome editing was observed with non-tagged Cas9 in previous ReMOT studies. I speculate that the large difference in genome editing efficiency between this study and previous attempts are probably due to the difference in the preparation of Cas9 and doses of Cas9 injected. In previous studies, Cas9 was purified only by a single step of affinity chromatography, which might have led to a product contaminated with undesired materials. Although commercial Cas9 was tested in the jewel wasp *N. vitripennis* (Chaverra-Rodriguez et al., 2018), the dose used was much lower than that used in this study (0.36 vs. 3.3 μg/μL in injection solution). To examine this view, I tested a serial dilution of Cas9 RNPs in *T. castaneum* and found a clear trend showing that decreased doses of Cas9 RNPs result in the decreased genome editing efficiency (Figure 3.6B and C). I thus propose using relatively high doses of commercial Cas9 when implementing my method to other species.

A

Company	Stage of injection	EER	Females injected	Survival rates	Screened G_0	G_0 edited animals		Genome editing efficiency (GEF)
						white	mosaic	
IDT	4 days AE	-	73	100%	63	25	7	50.8%
		-	36	97.2%	54	12	5	31.5%
Sigma-Aldrich	4 days AE	-	59	100%	22	3	3	27.3%
		-	76	98.7%	55	14		25.5%
FUJIFILM Wako	4 days AE	-	73	98.6%	101	14	10	23.8%
		-	78	100%	29	6	1	24.1%
Fasmac	4 days AE	-	50	100%	22	6	1	31.8%

B

Conc. of Cas9 (IDT)	Stage of injection	EER	Females injected	Survival rates	Screened G_0	G_0 edited animals		Genome editing efficiency (GEF)
						white	mosaic	
3.3 µg/µL	4 days AE	-	73	100%	63	25	7	50.8%
		-	36	97.2%	54	12	5	31.5%
1.65 µg/µL	4 days AE	-	85	100%	37	1	7	21.6%
		-	59	100%	20	4	2	30.0%
0.83 µg/µL	4 days AE	-	65	100%	23	1	2	13.0%
		-	90	100%	43	2	3	11.6%
0.41 µg/µL	4 days AE	-	64	100%	38	3	5	21.1%
		-	80	100%	67	2	1	4.5%

C

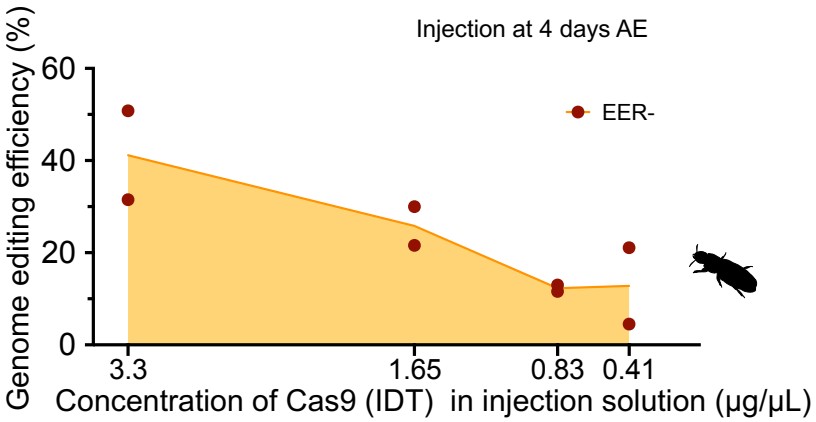

Figure 3.6. Performance of different Cas9 products and different doses of Cas9 in *Tribolium castaneum*

(A) Comparisons of Cas9 products from four vendors. Cas9 RNP solution containing 3.3 μg/μL Cas9 and 1.3 μg/μL sgRNA were injected into adult females of 4 days after adult eclosion (AE). (B) A dilution series of Cas9 RNPs (diluted by water, the molar ratio of Cas9 and sgRNA was fixed to be 1 : 2) were injected into females. (C) Genome editing efficiency shown in (B) was plotted against the concentration of Cas9 in injection solution. Each point represents the result of each replication.

The use of endosomal escape reagent

It has been reported that the efficiency of ReMOT-mediated genome editing can be improved with the use of endosomal escape reagents (EERs) that facilitate the release of Cas9 RNPs from the endosome to the cytosol (Chaverra-Rodriguez et al., 2018; Chaverra‐Rodriguez et al., 2020; Heu et al., 2020; Macias et al., 2020). Similarly, in my experiments, there were cases where the use of EER increased the efficiency (see Figures 3.1E and 3.2C). However, the effect of EER was not always clear, especially at some time points (see Figures 3.2C and 3.5B). Furthermore, the number of the eggs laid and/or hatched decreased in some cases (Figure 3.5B). As EERs often reduces survival rates and/or fecundity of the injected females (Chaverra-Rodriguez et al., 2018; Chaverra‐Rodriguez et al., 2020; Heu et al., 2020; Macias et al., 2020), their use in new target species needs empirical optimization through multiple rounds of experiments. Thus, I propose to use only two components, Cas9 and sgRNA, in my DIPA-CRISPR approach, which greatly simplifies the procedures for genome editing experiments.

A key parameter for DIPA-CRISPR

My experiments demonstrated that the most critical parameter for successful genome editing by DIPA-CRISPR is the stage of the adult females injected (Figure 3.7), which is also shown in the previous ReMOT studies. In the species tested in this study, the highest GEF was achieved with females actively undergoing vitellogenesis (Cornwell, 1968; Parthasarathy et al., 2010; Pascual et al., 1992; Treiblmayr et al., 2006). This finding, together with the fact that endocytosis results in the non-selective uptake of extracellular materials (Cooper et al., 2007), and that cultured insect ovaries can uptake and accumulate non-vitellogenin proteins (e.g., mouse IgG and bovine γ-globulin) (Kindle et al., 1988; Koller et al., 1989), suggests that the incorporation of Cas9 RNPs into vitellogenic oocytes occurs concomitantly with the

massive uptake of vitellogenins from the hemolymph (Raikhel and Dhadialla, 1992) (Figure 3.7A). Thus, a good knowledge of the vitellogenesis process in the target species can be an important prerequisite for using DIPA-CRISPR.

Like most insects, females of *T. castaneum* produce eggs continuously (i.e., they lay small number of eggs every day), whereas some insects such as cockroaches produce eggs in discrete batches (i.e., discontinuous reproductive cycle) (Figure 3.7B and 3.7C). Thus, vitellogenesis occurs almost throughout the adult stage in the former group, whereas at certain times in the latter group. Interestingly, I found a clear peak of GEF values in the former group. In *T. castaneum*, GEF values peaked on days 4 and 5 after emergence, after which the values decreased to a basal level (Figure 3.7C). Notably, this peak corresponds to the time of the onset of vitellogenesis that begins on day 4 after adult eclosion (Parthasarathy et al., 2010). The reason why these early stages give a very high efficiency is not clear, but my results would be helpful to design DIPA-CRISPR experiments in new target species.

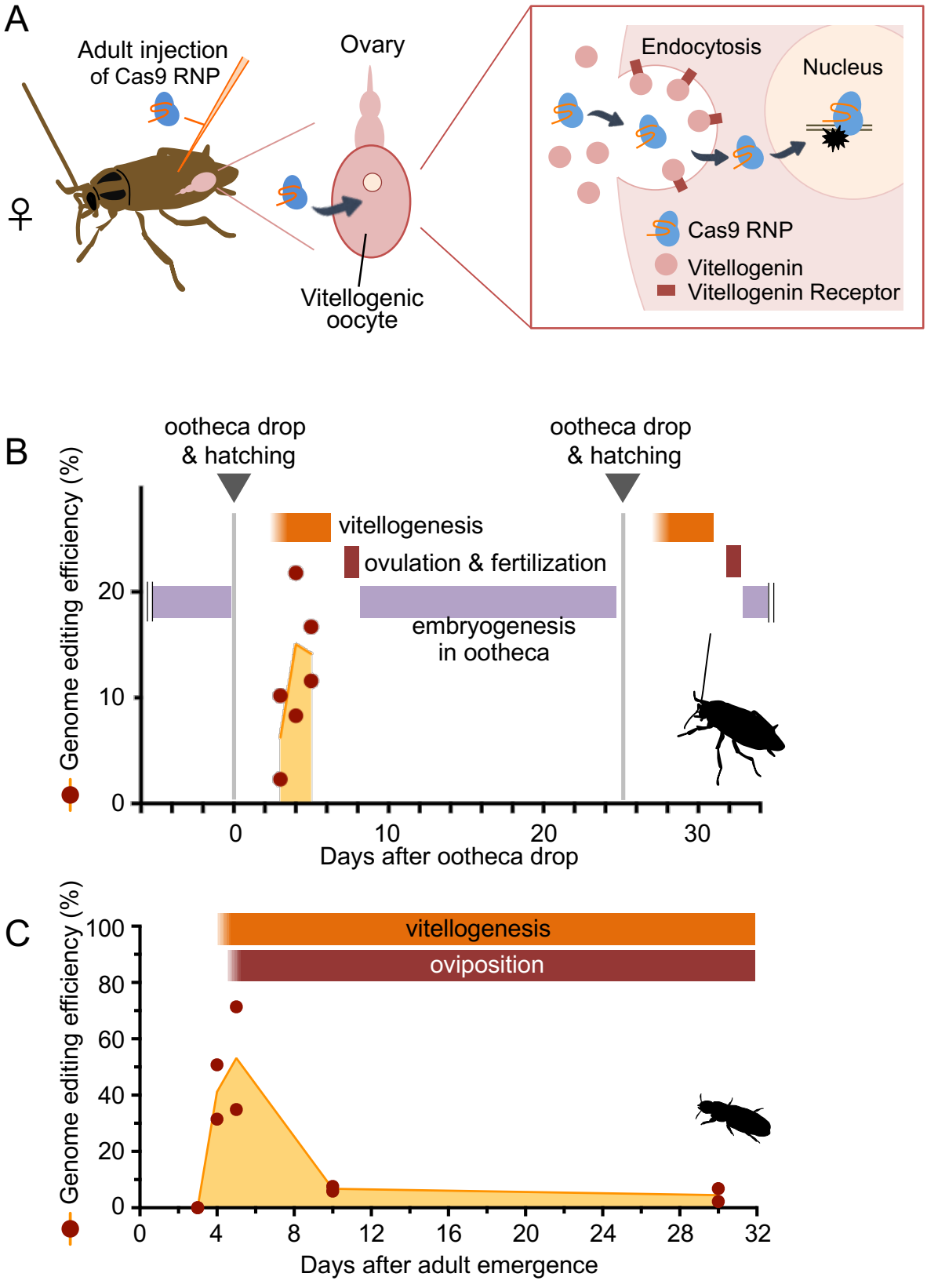
A
Adult injection
of Cas9 RNP
♀
Ovary
Vitellogenic
oocyte
Endocytosis
Nucleus
Cas9 RNP
Vitellogenin
Vitellogenin Receptor
B
ootheca drop
& hatching
ootheca drop
& hatching
vitellogenesis
ovulation & fertilization
embryogenesis
in ootheca
Genome editing efficiency (%)
0
10
20
0
10
20
30
Days after ootheca drop
C
vitellogenesis
oviposition
Genome editing efficiency (%)
0
20
40
60
80
100
0
4
8
12
16
20
24
28
32
Days after adult emergence

Figure 3.7. A schematic model and description of DIPA-CRISPR

(A) A schematic model of the uptake of Cas9 ribonucleoproteins (RNPs) by the oocyte. Vitellogenic oocytes massively uptake vitellogenins circulating in the hemolymph via receptor-mediated endocytosis (Raikhel and Dhadialla, 1992). Along with vitellogenin, injected Cas9 RNPs are likely non-selectively incorporated into the endosome of oocytes. Although the details of the process of endosomal escape are not clear, Cas9 RNPs then disrupt target genes in the nuclei of developing oocytes and/or fertilized embryos, producing gene-edited G_0 insects. (B and C) Relationship of genome editing efficiency and ovary development. Genome editing efficiencies are plotted against the stage of females of *B. germanica* (B) and *T. castaneum* (C). Each point represents the GEF value of each biological replication. My results suggest it is critical to set right timing of adult injection, depending on reproductive physiology of target species (i.e., continuous in *T. castaneum* vs. discontinuous in *B. germanica*). The timetable of ovary development is inferred from Parthasarathy et al. (2010), Pascual et al. (1992), and Treiblmayr et al. (2006).

DIPA-CRISPR as an accessible method for insect genome editing

My method requires only minimal equipment for adult injection, such as stereomicroscope and micromanipulator commonly used for larval/nymphal RNAi (Linz et al., 2014; Posnien et al., 2009). Thus, it could be readily implemented in any laboratory. Furthermore, the minimal requirement of reagents (i.e., Cas9 protein and sgRNA) makes this method highly practical and feasible.

As adult injection requires a much larger amount of injection solution compared to embryo microinjection (μL vs. nL scale per injection), the cost of reagents required for DIPA-CRISPR is expected to be higher than that for the conventional method. Thus, I calculated the cost of commercial Cas9 per recovered G_0 edited insects (Figure 3.8). When high doses of Cas9 RNPs (3.3 μg/μL Cas9 in injection solution) were injected at optimized stages, the cost was calculated to be 2.0–7.4 USD for *B. germanica* (Figure 3.8A) and 4.1–10.5 USD for *T. castaneum* (Figure 3.8B). I consider that this cost is at an accessible level given the minimal requirement of equipment and no need to produce in-house Cas9. On the other hand, my results in *T. castaneum* suggested that the cost could not be reduced by decreasing the dose of Cas9 RNPs (Figure 3.8C), because this decreases the total number of recovered mutants (Figure 3.6C). Thus, injection of relatively high doses of Cas9 RNPs would be a reasonable option, as this optimizes the chances of success without largely increasing the cost of reagents.

Due to its simplicity and accessibility, DIPA-CRISPR will greatly extend the application of genome editing technology to a wide variety of model and non-model insects, including global/local agricultural and medical pests whose genomes have not been manipulated in any way.

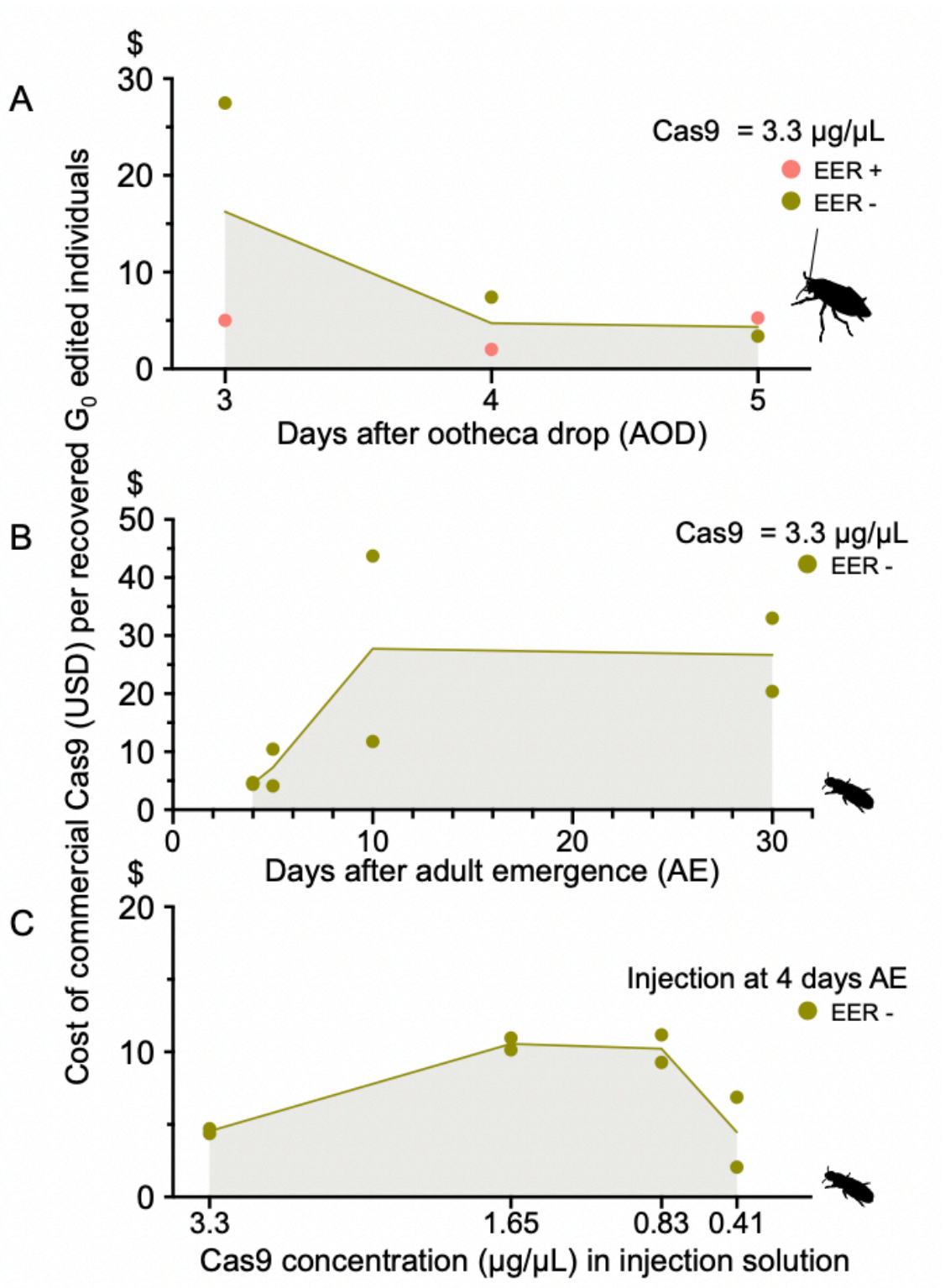

Figure 3.8. Cost of commercial Cas9 in DIPA-CRISPR

(A and B) Cost of commercial Cas9 (IDT, cat#10000735, 1.25 USD/μg) per recovered G_0 edited individuals was plotted against the time of injection for *B. germanica* (A) and *T. castaneum* (B). The results show that the cost can be significantly reduced by injecting at an appropriate timing in both species. Cost was calculated as follows: 1.25 (USD/μg) × amount (μg) of Cas9 injected per adult × total number of adults injected / total number of G_0 edited individuals recovered. Note that this calculation does not include the cost for sgRNA synthesis, as it greatly varies depending on the method (i.e., *in vitro* transcription or chemical synthesis). (C) Relationship of the cost of Cas9 and the concentration of Cas9 in injection solution in *T. castaneum*. The results shown in Figure 3.6 were used for calculation.

Limitations of this method

DIPA-CRISPR requires a good knowledge of ovary development in target species, since injected Cas9 RNPs utilize the process of vitellogenesis to be internalized into the oocyte. Thus, a precise staging of vitellogenic females may be crucial. However, this can be challenging in some species, given the diverse life histories and reproductive strategies in insects. Also, DIPA-CRISPR would not be applicable to species in which oogenesis proceeds without apparent vitellogenesis (e.g., aphids undergoing parthenogenetic reproduction) (Miura et al., 2003), or species in which vitellogenesis is mainly an ovarian autosynthetic process. For example, in the fruit fly *Drosophila melanogaster* and some higher Diptera, the major source of yolk proteins is the follicle cells surrounding the oocytes, but not the extraovarian fat body (Brennan et al., 1982; Houseman and Morrison, 1986). Further, the temporal and spatial range of 'patency', the opening of intercellular spaces between follicle cells that allows hemolymph-borne materials to reach the surface of oocytes (Raikhel and Dhadialla, 1992), is more limited in *D. melanogaster* than in most other species (Isasti-Sanchez et al., 2021; Row et al., 2021). To empirically establish the limits of my method in ovarian autosynthetic species, I tested it in *D. melanogaster* (Table 3.1), verifying that it does not work in them. Thus, my DIPA-CRISPR approach would not be directly applicable to some peculiar species that undergo a highly derived mode of vitellogenesis.

Gene	sgRNA	Stage of injection	EER	Females injected	Survival Rates	Screened G_0	G_0 edited animals		Genome editing efficiency (GEF)
							white	mosaic	
white	chemical synthesis	2 h AE	-	59	81.4%	212			0%
		2 h AE	-	29	96.6%	101			0%
		10 h AE	-	31	87.1%	2			0%
		10 h AE	-	26	96.2%	33			0%
		10 h AE	-	80	96.3%	270			0%
		24 h AE	-	61	85.2%	481			0%
		24 h AE	-	71	91.5%	426			0%
		2 d AE	-	47	53.2%	324			0%
		2 d AE	-	58	77.6%	437			0%
		4 d AE	-	53	60.4%	329			0%
		4 d AE	-	63	76.2%	421			0%
		7 d AE	-	62	66.1%	841			0%
		7 d AE	-	65	80.0%	573			0%
		Random	Chl 2 mM	113	93.1%	891			0%
	in vitro transcription	Random	-	71	91.5%	340			0%
		Random	Chl 0.5 mM	74	95.9%	417			0%
		Random	Chl 2 mM	70	88.6%	662			0%

Table 3.1. DIPA-CRISPR in *Drosophila melanogaster*

Cas9 ribonucleoprotein (RNP) solution containing 3.3 μg/μL Cas9 (IDT, Cat#1081059) and 1.3 μg/μL sgRNA (a mixture of sgRNA1 and sgRNA2) were injected into adult females of selected hours or days after adult emergence (AE), or females that were randomly chosen from vials (Random). sgRNAs were purchased (chemical synthesis) or synthesized by in vitro transcription. The injected females were pooled, and the results are from the eggs laid during the first 48 h after injection. EER, presence or absence (-) of an endosomal escape reagent chloroquine (Chl) in injection solution.

3.4. References

Belles, X., 2020. Insect Metamorphosis: From Natural History to Regulation of Development and Evolution (Academic Press).

Brennan, M.D., Weiner, A.J., Goralski, T.J., Mahowald, A.P., 1982. The follicle cells are a major site of vitellogenin synthesis in *Drosophila melanogaster*. Dev. Biol. 89, 225–236. https://doi.org/10.1016/0012-1606(82)90309-8

Chaverra-Rodriguez, D., Macias, V.M., Hughes, G.L., Pujhari, S., Suzuki, Y., Peterson, D.R., Kim, D., McKeand, S., Rasgon, J.L., 2018. Targeted delivery of CRISPR-Cas9 ribonucleoprotein into arthropod ovaries for heritable germline gene editing. Nat. Commun. 9, 1–11. https://doi.org/10.1038/s41467-018-05425-9

Chaverra-Rodriguez, D., Dalla Benetta, E., Heu, C.C., Rasgon, J.L., Ferree, P.M., Akbari, O.S., 2020. Germline mutagenesis of *Nasonia vitripennis* through ovarian delivery of CRISPR-Cas9 ribonucleoprotein. Insect Mol. Biol. 29, 569‐577. https://doi.org/10.1111/imb.12663

Ciudad, L., Piulachs, M.D., Bellés, X., 2006. Systemic RNAi of the cockroach vitellogenin receptor results in a phenotype similar to that of the *Drosophila yolkless* mutant. FEBS J. 273, 325–335. https://doi.org/10.1111/j.1742-4658.2005.05066.x

Cooper, G.M., Hausman, R.E., 2007. The Cell: A Molecular Approach (ASM Press).

Cornwell, P.B., 1968. The cockroach. Volume 1. A laboratory and insect and an industrial pest (Hutchinson Press).

Daimon, T., Uchibori, M., Nakao, H., Sezutsu, H., Shinoda, T., 2015. Knockout silkworms reveal a dispensable role for juvenile hormones in holometabolous life cycle. Proc. Natl. Acad. Sci. 112, E4226–E4235. https://doi.org/10.1073/pnas.1506645112

Dermauw, W., Jonckheere, W., Riga, M., Livadaras, I., Vontas, J., Van Leeuwen, T., 2020. Targeted mutagenesis using CRISPR-Cas9 in the chelicerate herbivore *Tetranychus urticae*. Insect Biochem. Mol. Biol. 120, 103347. https://doi.org/10.1016/j.ibmb.2020.103347

Doudna, J.A., Charpentier, E., 2014. The new frontier of genome engineering with CRISPR-Cas9. Science 346. https://doi.org/10.1126/science.1258096

Gantz, V.M., Akbari, O.S., 2018. Gene editing technologies and applications for insects. Curr. Opin. Insect Sci. 28, 66–72. https://doi.org/10.1016/j.cois.2018.05.006

Gilles, A.F., Schinko, J.B., Averof, M., 2015. Efficient CRISPR-mediated gene targeting and transgene replacement in the beetle *Tribolium castaneum*. Development 142, 2832–2839. https://doi.org/10.1242/dev.125054

Grubbs, N., Haas, S., Beeman, R.W., Lorenzen, M.D., 2015. The ABCs of eye color in *Tribolium castaneum*: Orthologs of the Drosophila *white*, *scarlet*, and *brown* genes. Genetics 199, 749–759. https://doi.org/10.1534/genetics.114.173971

Harrison, M.C., Jongepier, E., Robertson, H.M., Arning, N., Bitard-Feildel, T., Chao, H., Childers, C.P., Dinh, H., Doddapaneni, H., Dugan, S., Gowin, J., Greiner, C., Han, Y., Hu, H., Hughes, D.S.T., Huylmans, A.K., Kemena, C., Kremer, L.P.M., Lee, S.L., Lopez-Ezquerra, A., Mallet, L., Monroy-Kuhn, J.M., Moser, A., Murali, S.C., Muzny, D.M., Otani, S., Piulachs, M.D., Poelchau, M., Qu, J., Schaub, F., Wada-Katsumata, A., Worley, K.C., Xie, Q., Ylla, G., Poulsen, M., Gibbs, R.A., Schal, C., Richards, S., Belles, X., Korb, J., Bornberg-Bauer, E., 2018. Hemimetabolous genomes reveal molecular basis of termite eusociality. Nat. Ecol. Evol. 2, 557–566. https://doi.org/10.1038/s41559-017-0459-1

Heu, C.C., McCullough, F.M., Luan, J., Rasgon, J.L., 2020. CRISPR-Cas9-based genome editing in the silverleaf whitefly (*Bemisia tabaci*). CRISPR J. 3, 89–96.

https://doi.org/10.1089/crispr.2019.0067

Hill, J.T., Demarest, B.L., Bisgrove, B.W., Su, Y.C., Smith, M., Yost, H.J., 2014. Poly peak parser: Method and software for identification of unknown indels using sanger sequencing of polymerase chain reaction products. Dev. Dyn. 243, 1632–1636. https://doi.org/10.1002/dvdy.24183

Houseman, J.G., Morrison, P.E., 1986. Absence of Female-Specific Protein in the. Arch. Insect Biochem. Physiol. 3, 205–213.

Hwang, W.Y., Fu, Y., Reyon, D., Maeder, M.L., Tsai, S.Q., Sander, J.D., Peterson, R.T., Yeh, J.R.J., Joung, J.K., 2013. Efficient genome editing in zebrafish using a CRISPR-Cas system. Nat. Biotechnol. 31, 227–229. https://doi.org/10.1038/nbt.2501

Isasti-Sanchez, J., Münz-Zeise, F., Lancino, M., Luschnig, S., 2021. Transient opening of tricellular vertices controls paracellular transport through the follicle epithelium during *Drosophila* oogenesis. Dev. Cell 56, 1083-1099.e5. https://doi.org/10.1016/j.devcel.2021.03.021

Kindle, H., König, R., Lanzrein, B., 1988. In vitro uptake of vitellogenin by follicles of the cockroach *Nauphoeta cinerea*: Comparison of artificial media with haemolymph media and role of vitellogenin concentration and of juvenile hormone. J. Insect Physiol. 34, 541–548. https://doi.org/10.1016/0022-1910(88)90196-5

Koller, C.N.., Dhadialla, T.S., Raikhel, A.S., 1989. Selective endocytosis of vitellogenin by oocytes of the mosquito, *Aedes aegypti*: An in vitro study. Insect Biochem. 19, 693–702. https://doi.org/10.1016/0020-1790(89)90106-6

Li, A., Sadasivam, M., Ding, J.L., 2003. Receptor-ligand interaction between vitellogenin receptor (VtgR) and vitellogenin (Vtg), implications on low density lipoprotein receptor and apolipoprotein B/E. J. Biol. Chem. 278, 2799–2806. https://doi.org/10.1074/jbc.m205067200

Linz, D.M., Clark-Hachtel, C.M., Borràs-Castells, F., Tomoyasu, Y., 2014. Larval RNA interference in the red flour beetle, *Tribolium castaneum*. J. Vis. Exp. 1–8. https://doi.org/10.3791/52059

Lorenzen, M.D., Brown, S.J., Denell, R.E., Beeman, R.W., 2002. Cloning and characterization of the *Tribolium castaneum* eye-color genes encoding tryptophan oxygenase and kynurenine 3-monooxygenase. Genetics 160, 225–234. https://doi.org/10.1093/genetics/160.1.225

Macias, V.M., McKeand, S., Chaverra-Rodriguez, D., Hughes, G.L., Fazekas, A., Pujhari, S., Jasinskiene, N., James, A.A., Rasgon, J.L., 2020. Cas9-Mediated Gene-Editing in the Malaria Mosquito *Anopheles stephensi* by ReMOT Control. G3 Genes, Genomes, Genet. 10, 1353–1360. https://doi.org/10.1534/g3.120.401133

Matthews, B.J., Vosshall, L.B., 2020. How to turn an organism into a model organism in 10 “easy” steps. J. Exp. Biol. 223, jeb218198. https://doi.org/10.1242/jeb.218198

Mclaughlin, J.M., Bratu, D.P., 2015. *Drosophila melanogaster* Oogenesis: An Overview. Methods Mol. Biol. 1328, 1–20. https://doi.org/10.1007/978-1-4939-2851-4_1

Meisel, R.P., Delclos, P.J., Wexler, J.R., 2019. The X chromosome of the German cockroach, *Blattella germanica*, is homologous to a fly X chromosome despite 400 million years divergence. BMC Biol. 17, 1–14. https://doi.org/10.1186/s12915-019-0721-x

Misof, B., Liu, S., Meusemann, K., Peters, R.S., Donath, A., Mayer, C., Frandsen, P.B., Ware, J., Flouri, T., Beutel, R.G., Niehuis, O., Petersen, M., Izquierdo-Carrasco, F., Wappler, T., Rust, J., Aberer, A.J., Aspöck, U., Aspöck, H., Bartel, D., Blanke, A., Berger, S., Böhm, A., Buckley, T.R., Calcott, B., Chen, J., Friedrich, F., Fukui, M., Fujita, M., Greve, C., Grobe, P., Gu, S., Huang, Y., Jermiin, L.S., Kawahara, A.Y., Krogmann, L., Kubiak, M., Lanfear, R., Letsch, H., Li, Yiyuan, Li, Z., Li, J., Lu, H., Machida, R., Mashimo, Y., Kapli, P., McKenna, D.D., Meng, G., Nakagaki, Y., Navarrete-Heredia, J.L., Ott, M., Ou,

Y., Pass, G., Podsiadlowski, L., Pohl, H., Reumont, B.M. von, Schütte, K., Sekiya, K., Shimizu, S., Slipinski, A., Stamatakis, A., Song, W., Su, X., Szucsich, N.U., Tan, M., Tan, X., Tang, M., Tang, J., Timelthaler, G., Tomizuka, S., Trautwein, M., Tong, X., Uchifune, T., Walzl, M.G., Wiegmann, B.M., Wilbrandt, J., Wipfler, B., Wong, T.K.F., Wu, Q., Wu, G., Xie, Y., Yang, S., Yang, Q., Yeates, D.K., Yoshizawa, K., Zhang, Q., Zhang, R., Zhang, W., Zhang, Yunhui, Zhao, J., Zhou, C., Zhou, L., Ziesmann, T., Zou, S., Li, Yingrui, Xu, X., Zhang, Yong, Yang, H., Wang, Jian, Wang, Jun, Kjer, K.M., Zhou, X., 2014. phylogenomics resolves the timing and pattern of insect evolution. Science 346, 763–767. https://doi.org/10.1126/science.aaa5460

Miura, T., Braendle, C., Shingleton, A., Sisk, G., Kambhampati, S., Stern, D.L., 2003. A comparison of parthenogenetic and sexual embryogenesis of the pea aphid *Acyrthosiphon pisum* (Hemiptera: Aphidoidea). J. Exp. Zool. Part B Mol. Dev. Evol. 295, 59–81. https://doi.org/10.1002/jez.b.3

Murakami, Y., Horibe, T., Kinoshita, M., 2019. Development of an efficient bioreactor system for delivering foreign proteins secreted from liver into eggs with a vitellogenin signal in medaka *Oryzias latipes*. Fish. Sci. 85, 677–685. https://doi.org/10.1007/s12562-019-01320-4

Parthasarathy, R., Sheng, Z., Sun, Z., Palli, S.R., 2010. Ecdysteroid regulation of ovarian growth and oocyte maturation in the red flour beetle, *Tribolium castaneum*. Insect Biochem. Mol. Biol. 40, 429–439. https://doi.org/10.1016/j.ibmb.2010.04.002

Pascual, N., Cerdá, X., Benito, B., Tomás, J., Piulachs, M., and Bellés, X., 1992. Ovarian ecdysteroid levels and basal oöcyte development during maturation in the cockroach *Blattella germanica* (L.). J. Insect Physiol. 38, 339–348. https://doi.org/10.1016/0022-1910(92)90058-l.

Posnien, N., Schinko, J., Grossmann, D., Shippy, T.D., Konopova, B., Bucher, G., 2009.

RNAi in the red flour beetle (*Tribolium*). Cold Spring Harb. Protoc. 4, 1–9. https://doi.org/10.1101/pdb.prot5256

Quan, G.X., Kim, I., Kômoto, N., Sezutsu, H., Ote, M., Shimada, T., Kanda, T., Mita, K., Kobayashi, M., Tamura, T., 2002. Characterization of the kynurenine 3-monooxygenase gene corresponding to the *white egg 1* mutant in the silkworm *Bombyx mori*. Mol. Genet. Genomics 267, 1–9. https://doi.org/10.1007/s00438-001-0629-2

Raikhel, A.S., Dhadialla, T.S., 1992. Accumulation of yolk proteins in insect oocytes. Annu. Rev. Entomol. 37, 217–251. https://doi.org/10.1146/annurev.ento.37.1.217

Ren, X., Yang, Z., Xu, J., Sun, J., Mao, D., Hu, Y., Yang, S.J., Qiao, H.H., Wang, X., Hu, Q., Deng, P., Liu, L.P., Ji, J.Y., Li, J.B., Ni, J.Q., 2014. Enhanced specificity and efficiency of the CRISPR/Cas9 system with optimized sgRNA parameters in *Drosophila*. Cell Rep. 9, 1151–1162. https://doi.org/10.1016/j.celrep.2014.09.044

Row, S., Huang, Y.C., Deng, W.M., 2021. Developmental regulation of oocyte lipid intake through 'patent' follicular epithelium in *Drosophila melanogaster*. iScience 24, 102275. https://doi.org/10.1016/j.isci.2021.102275

Shirai, Y., Daimon, T., 2020. Mutations in *cardinal* are responsible for the *red-1* and *peach* eye color mutants of the red flour beetle *Tribolium castaneum*. Biochem. Biophys. Res. Commun. 529, 372–378. https://doi.org/10.1016/j.bbrc.2020.05.214

Tamura, T., Thibert, C., Royer, C., Kanda, T., Abraham, E., Kamba, M., Komoto, N., Thomas, J.L., Mauchamp, B., Chavancy, G., Shirk, P., Fraser, M., Prudhomme, C., Couble, P., 2000. Germline transformation of the silkworm *Bombyx mori* L. using a *piggyBac* transposon-derived vector. Nat. Biotechnol. 18, 559. https://doi.org/10.1038/75446

Treiblmayr, K., Pascual, N., Piulachs, M.D., Keller, T., Belles, X., 2006. Juvenile hormone titer versus juvenile hormone synthesis in female nymphs and adults of the German cockroach, *Blattella germanica*. J. Insect Sci. 6, 1–7.

https://doi.org/10.1673/031.006.4301

Chapter 4
DIPA-CRISPR genome editing in mosquitoes

4.1 Introduction

The development of genome editing tools has enabled sophisticated genome engineering in insects (Gantz and Akbari, 2018; Matthews and Vosshall, 2020). Current methods for genome editing in insects rely on embryonic microinjection at the preblastoderm stage, which requires expensive equipment and high technical skill. These limit the application of genome editing methods to a wide variety of insect species. For example, microinjection into an early embryo is very difficult or virtually impossible in species that lay their eggs inside their prey (e.g., parasitoid wasps), produce live larvae instead of eggs (e.g., viviparous aphids and flesh flies), or produce a hard egg case encapsulating their eggs (e.g., cockroaches).

Recently, an alternative method known as “direct parental” CRISPR (DIPA-CRISPR) was developed, which enables genome editing by simple adult injection (Shirai et al., 2022). This technique only requires two components: commercial Cas9 protein and single-guide RNA (sgRNA). Cas9 ribonucleoproteins (RNPs) injected into adult females are incorporated into developing oocytes from the hemolymph along with yolk protein precursors, thereby introducing heritable mutations into the oocytes. I demonstrated previously that DIPA-CRISPR enables highly efficient genome editing in the German cockroach *Blattella germanica* and the red flour beetle *Tribolium castaneum* (Shirai et al., 2022).

Despite its simplicity, the applicability of DIPA-CRISPR to a wider range of insects has not been fully explored. There are three distinct organizations of insect ovaries, which include panoistic, telotrophic meroistic, and polytrophic meroistic ovaries (Mclaughlin and

Bratu, 2015). Although I showed that DIPA-CRISPR is applicable to insects with panositic (*B. germanica*) and telotrophic (*T. castaneum*) ovaries, it is unclear whether it is also applicable to insects with the most derived, polytrophic meroistic ovaries. In this study, I evaluated DIPA-CRISPR in the yellow fever mosquito *Aedes aegypti* (L.) (Diptera: Culicidae), which has polytrophic ovaries. I provide evidence that DIPA-CRISPR works in *A. aegypti*, suggesting that this simple, accessible method can be applied to insects with all three types of ovaries.

4.2 Materials and Methods

Insects

The *A. aegypti* strain was derived from the Liverpool strain and was kindly provided by Dr. Ryuichiro Maeda (Obihiro University of Agriculture and Veterinary Medicine). Eggs were obtained by a standard procedure and incubated in reverse osmosis (RO) water. The hatched first instar larvae were transferred to a plastic container and provided RO water and daily fish food (Hikari, Kyorin Co., Ltd., Japan). The larvae were maintained in an insectary room at 27 ℃, and the water was refreshed every 2–3 days. Pupae were collected in a plastic cup and placed in a cage (bottom 27 cm × 27 cm, top 25 cm × 25 cm, height 27 cm) with a 50-ml glass flask containing 10% sucrose solution with an inserted filter paper (Whatman, USA). The cage in which the emerged adults were reared was maintained in an incubator (Panasonic Co., Japan) at 27 ℃ with humidity over 90% in a standard 12 h:12 h light:dark cycle. The sucrose solution was changed every 3–4 days. For injection experiments, the adult females were fed mouse blood and separated from males prior to injection.

Preparation of Cas9-sgRNA RNPs

sgRNAs targeting *A. aegypti kmo* (GenBank: NC_035108.1) were synthesized as previously described (Shirai et al., 2022; Shirai and Daimon, 2020). Briefly, annealed oligo DNA was cloned into the BsaI site of the pDR274 vector (Hwang et al., 2013). After linearization with DraI, the vector was used as a template for in vitro transcription using the T7 RiboMAX Express Large Scale RNA Production System (Promega). The synthesized sgRNAs were extracted with phenol (pH 4–5):chloroform:isoamyl alcohol (125:24:1) (Sigma), precipitated with isopropanol, and dissolved in RNase-free water. Commercial Cas9 protein was purchased from IDT (Alt-R S.p. Cas9 Nuclease V3). Cas9 protein and sgRNAs were mixed at a molar ratio of approximately 1:2 and incubated for 10–15 min at room temperature to allow Cas9 RNP formation. The target sequences of the sgRNAs are (5'- to -3'): AAGACCAGGCCTCAATCGT for sgRNA1 and CGGCAAGGCGGTGATCAT for sgRNA2.

Adult injections and screening

Injections were performed using a glass capillary needle equipped with an IM 300 Microinjector (NARISHIGE). Females were anesthetized on ice. Approximately 200 nL of the Cas9 RNP solution containing 3.3 μg/μL Cas9 (IDT) and 1.3 μg/μL sgRNAs (a mixture of sgRNA1 and sgRNA2) was injected into the thorax of the adult females. The females were subsequently grouped in a cage (bottom 15 cm × 15 cm, top 15 cm × 15 cm, height 15 cm). The eggs were laid onto filter paper soaked in RO water beginning 2 days after blood-feeding. The G_0 progeny were collected for 3–4 days after the paper was set. The eye colors of the G_0 generation were examined at the pupal or adult stage. For the screening based on genotyping experiments, I randomly selected 282 individuals from the G_0 population of each experimental condition.

Genotyping

Genomic DNAs were extracted individually as previously described (Daimon et al., 2015). Genomic PCR was per- formed using KOD FX Neo (TOYOBO). Mutations were screened by analyzing the PCR products from a heteroduplex mobility assay (HMA) using the Mul- tiNA Microchip Electrophoresis System (MCE-202, Shimadzu). Primer sequences for HMA are (5'- to -3'): ATTGGTCGTGAGCGGTTGG and GTACAATCCTCGAATCCGGCATTC . Primer sequences for Sanger sequencing are (5' - to -3'): GCA CTT GGA CGG TGA CGC TG and GTA CAA TCC TCG AAT CCG GCA TTC.

Ethics statement

This study was carried out in accordance with the Guideline for Laboratory Animals of The Jikei University School of Medicine and the Fundamental Guidelines for Proper Conduct of Animal Experiment and Related Activities in Academic Research Institutions under the jurisdiction of the Japanese Ministry of Education, Culture, Sports, Science, and Technology. The protocol was approved by the Committee on the Animal Experiments of The Jikei University School of Medicine (Permit Number 2020–007).

4.3 Results

Target gene for DIPA-CRISPR in *A. aegypti*

To evaluate the efficiency of DIPA-CRISPR in *A. aegypti*, I targeted the kynurenine 3-monooxygenase (*kmo*) gene, which is essential for eye pigmentation and has been used as a target in previous studies of this species. I attempted to use the same sgRNAs as that in previous studies (sgRNA460 and sgRNA519* in Basu et al., 2015 and Chaverra-Rodriguez et

al., 2018); however I found that there was a SNP in the target site of sgRNA519* in my strain (data not shown). Therefore, I used two sgRNAs: one was newly designed (sgRNA1) and the other was identical to sgRNA460 (Basu et al., 2015; Chaverra-Rodriguez et al., 2018) (sgRNA2) (Fig. 4.1A).

In *A. aegypti*, synchronous egg development is regulated by blood-feeding (Raikhel and Dhadialla 1992). Because the highest genome editing efficiency was achieved by injecting females at the vitellogenic stage in *B. germanica* and *T. castaneum* (Shirai et al., 2022), I evaluated three time points around the onset of vitellogenesis in *A. aegypti*, specifically, 6, 24, and 48 h after blood-feeding (ABF).

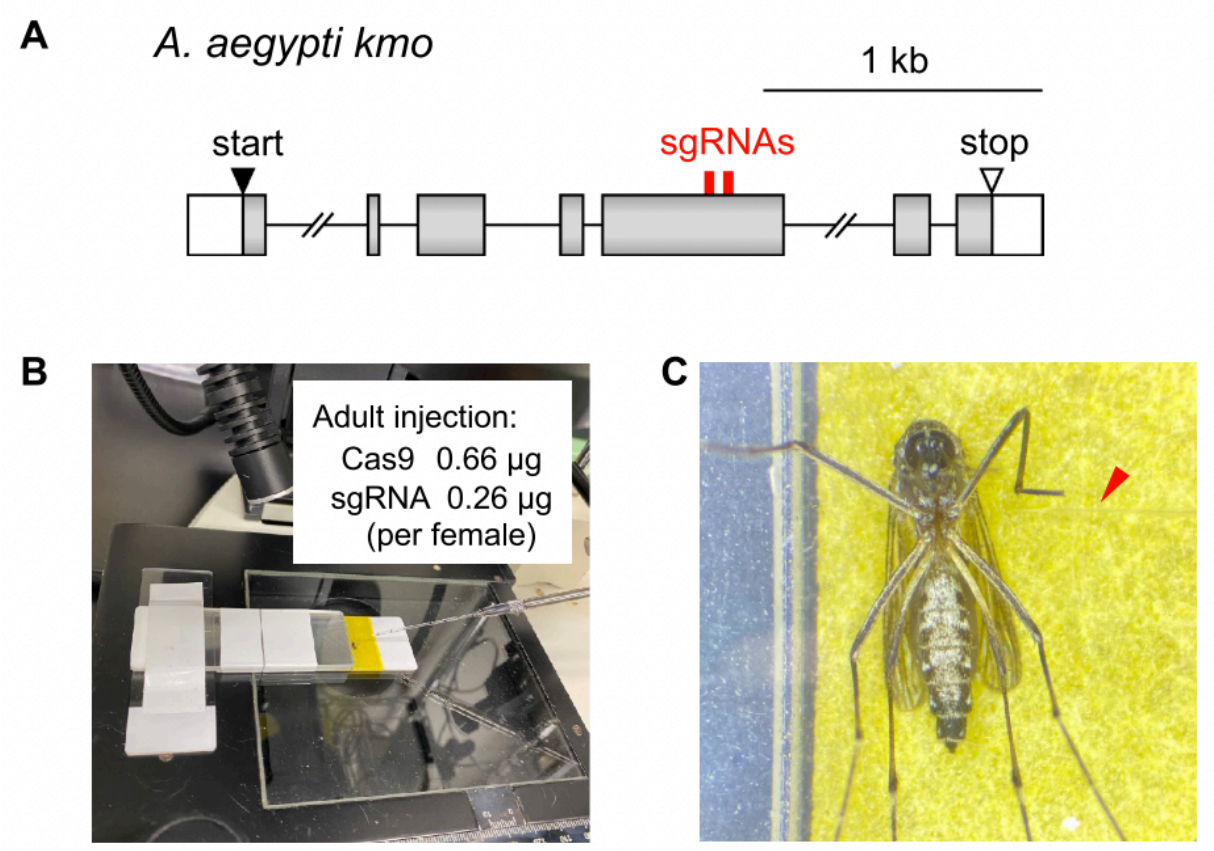

Figure 4.1. DIPA-CRISPR in *Aedes aegypti*

(A) DIPA-CRISPR target sites of the *A. aegypti kmo* gene (NC_035108.1). The red box indicates the sgRNA sites. (B) Adult injection in *A. aegypti*. (C) Enlarged images of injected *A. aegypti*. Females were injected intrathoracically. An arrowhead indicates the glass capillary needle.

DIPA-CRISPR experiments in *A. aegypti*

I prepared a mixture of commercial Cas9 and the two sgRNAs targeting *kmo* and injected it into females at selected hours ABF (Fig. 4.1B and 4.1C). When I screened the eye colors of the progeny (generation zero, G_0), I was able to recover a white-eyed G_0 individual from the progeny of females injected at 24 h ABF (Fig. 4.2A). To verify that the desired genome editing events had occurred in this white-eyed animal, I performed genomic PCR and observed two DNA bands, which indicated the presence of a large deletion allele (Fig. 4.2B). Sanger sequencing of the subcloned PCR products revealed that there were multiple types of edited alleles in this white-eyed animal, including the large deletion allele (Fig. 4.2C). Of note, all 15 sequenced clones carried insertions and/or deletions; thus, it is likely that almost all cells of this G_0 white mutant carried edited alleles. Because *kmo* is an autosomal gene, the recovery of the white-eyed animal indicates that Cas9 RNPs induced biallelic (i.e., both maternal and paternal) mutations in this animal.

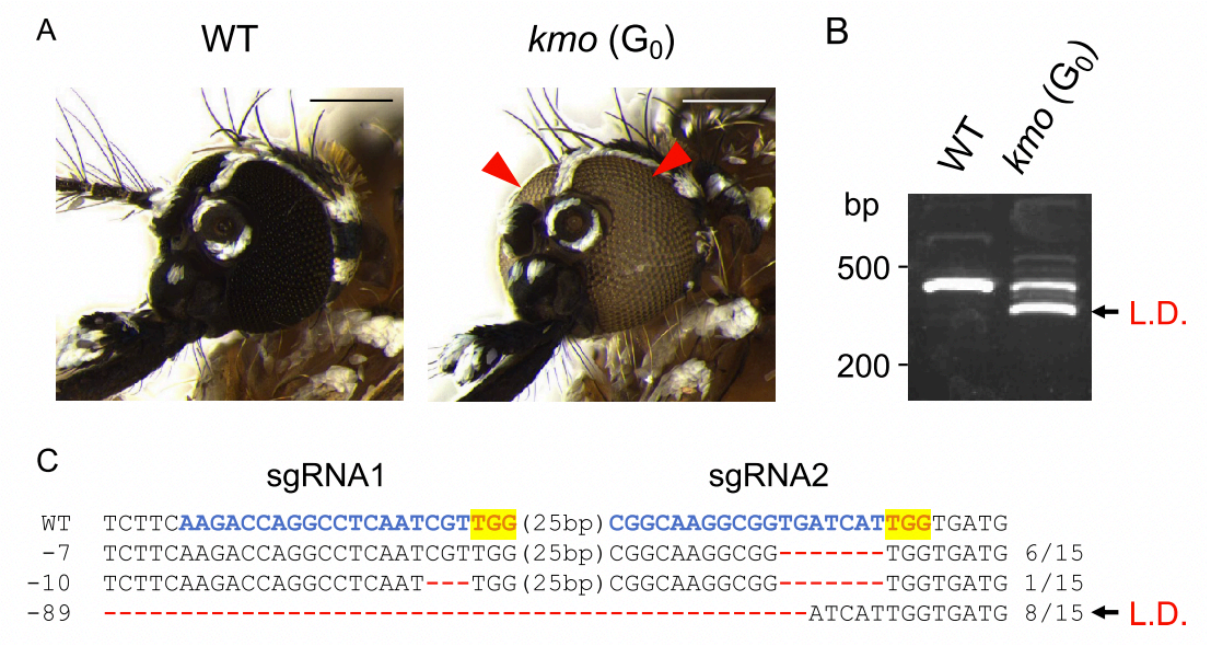

Figure 4.2. A white-eyed G_0 individual

(A) A recovered white-eyed G_0 adult. Arrowheads indicate white eyes. Scale bars, 250 μm. (B) Detection of a large genomic deletion in the white-eyed G_0 animal by genomic PCR. (C) The DNA sequences of the edited alleles in the white-eyed G_0 animal. Blue letters represent sgRNAs and highlighted orange letters indicate PAM sequences. L.D. indicates the induced large deletion.

Screening of edited animals by genotyping

To further screen for mosquitoes with edited alleles without detectable external phenotypes, 288 G_0 individuals from each experimental condition were randomly selected and subjected to HMA. I obtained one edited animal from the batch injected at 6 h ABF [genome editing efficiency (GEF) = 0.3%] and 10 animals from the batch injected at 24 h ABF, respectively (GEF = 3.5%) (Fig. 4.3A and Table 4.1). In contrast, I was unable to recover any gene-edited animals from the batch injected at 48 h ABF (Table 4.1).

To determine the nucleotide sequences of the edited alleles, two individuals (#3 and #8 in Fig. 4.3A) were subjected to Sanger sequencing. For individual #3, two of the five subclones contained a 10-bp deletion at the site of sgRNA2 (Fig. 4.3B). In the eight subclones from individual #8, one contained a 10-bp deletion, two had an 18-bp deletion, and one harbored a 24-bp deletion (Fig. 4.3B). These results indicate that both sgRNAs exhibited genome editing activity and that multiple genome editing events occurred in the oocytes before and/or after fertilization. Importantly, I show that the injection at 24 h ABF exhibited the highest GEF (GEF = 3.5%) (Table 4.1), which corresponds to the time of vitellogenesis (Koller et al., 1989; Koller and Raikhel, 1991).

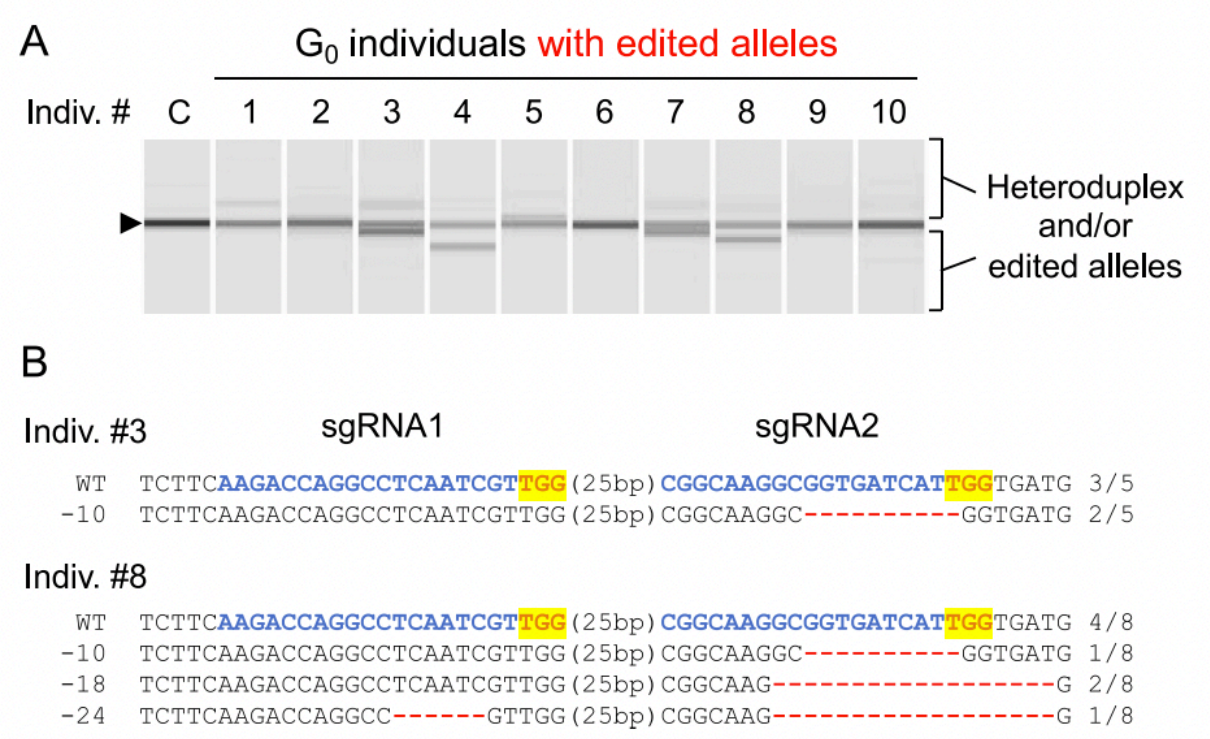

Figure 4.3. The results of genotyping in G_0 individuals

(A) The results of the heteroduplex mobility assay (HMA) in G_0 individuals carrying edited alleles. An arrowhead indicates the band from the wild-type allele. (B) The DNA sequences of the mutant alleles from individuals #3 and #8. Blue letters indicate sgRNAs and highlighted orange letters indicate PAM sequences.

Protein	Time of injection ABF[a]	Injected females	Survival rates[b] (%)	Screened G_0 by genotyping	G_0 with edited alleles	GEF[c] (%)
Cas9 (IDT)	6 h ABF	40	82.5	288	1	0.3
	24 h ABF	40	75	288	10	3.5
	48 h ABF	41	100	288	0	0

[a]*ABF* after blood-feeding

[b]Survival rates were calculated between 1 and 3 days post injection

[c]*GEF* genome editing efficiency

Table 4.1. The efficiency of DIPA-CRISPR in *Aedes aegypti*

4.4 Discussion

In the present study, I successfully adapted DIPA-CRISPR to the yellow fever mosquito *A. aegypti*, which contains the derived polytrophic meroistic ovaries. I also found that the 24 h ABF injection exhibited the highest genome editing efficiency (Table 4.1). In *A. aegypti*, the uptake of yolk protein precursors peaks between 24 and 30 h ABF, followed by a rapid decline and a cessation of uptake by 36 h (Koller et al., 1989; Koller and Raikhel, 1991). Therefore, the peak of GEF values corresponds well with the time of the vitellogenesis in *A. aegypti*. Similar results were obtained in *B. germanica* and *T. castaneum*, in which the highest GEF values were achieved in females undergoing vitellogenesis. Therefore, my results clearly demonstrate that a key parameter for DIPA-CRISPR is the stage at which the females are injected.

There is another method of genome editing by adult injection, known as Receptor-Mediated Ovary Transduction of Cargo (ReMOT) (Chaverra-Rodriguez et al., 2018). Thus far, ReMOT has been applied to several species, including mosquitoes (Chaverra-Rodriguez et al., 2018; Li et al., 2021; Macias et al., 2020) wasps (Chaverra-Rodriguez et al., 2020), beetles (Shirai and Daimon, 2020), whiteflies (Heu et al., 2020), and a non-insect tick species (Sharma et al., 2022). However, this method has some limitations, such as the need to produce recombinant Cas9 protein fused to peptide ligands. This facilitates ovary transduction and the use of endosomal escape reagents (EERs) that are thought to facilitate the release of Cas9 RNPs from the endosome into the cytosol. In the previous ReMOT study, the same target gene *kmo* was disrupted in the same species (Chaverra-Rodriguez et al., 2018), and the highest GEF was 2.4% when the maternal alleles were disrupted and screening was based on eye color phenotypes. Although I cannot directly

compare the efficiency of two different studies with different screening strategies, I suggest that the efficiency of my DIPA-CRISPR approach (GEF = 3.5%) was at a practical level. Because of the simplicity of the procedure, which eliminates the need for engineering, preparation of recombinant Cas9 proteins, and the use and optimization of EERs, DIPA-CRISPR would be a more feasible and accessible approach for genome editing in mosquitoes.

I previously demonstrated that DIPA-CRISPR enables efficient genome editing in insects with panositic (*B. germanica*) and telotrophic (*T. castaneum*) ovaries. Therefore, my successful genome editing in mosquitoes using DIPA-CRISPR strongly suggests that this approach can be applied to all three types of ovaries. In addition, genome editing was achieved in the spider mite (Dermauw et al., 2020) by adult injection of non-tagged Cas9 and sgRNA. I anticipate that DIPA-CRISPR will be extended to a wide variety of non-model insects and other arthropods as a research tool for answering fundamental biological questions as well as for the control of agricultural and medical pests.

4.5. References

Basu, S., Aryan, A., Overcash, J.M., Samuel, G.H., Anderson, M.A.E., Dahlem, T.J., Myles, K.M., Adelman, Z.N., 2015. Silencing of end-joining repair for efficient site-specific gene insertion after TALEN/CRISPR mutagenesis in *Aedes aegypti*. Proc. Natl. Acad. Sci. U. S. A. 112, 4038–4043. https://doi.org/10.1073/pnas.1502370112

Chaverra-Rodriguez, D., Macias, V.M., Hughes, G.L., Pujhari, S., Suzuki, Y., Peterson, D.R., Kim, D., McKeand, S., Rasgon, J.L., 2018. Targeted delivery of CRISPR-Cas9 ribonucleoprotein into arthropod ovaries for heritable germline gene editing. Nat.

Commun. 9, 1–11. https://doi.org/10.1038/s41467-018-05425-9

Chaverra-Rodriguez, D., Dalla Benetta, E., Heu, C.C., Rasgon, J.L., Ferree, P.M., Akbari, O.S., 2020. Germline mutagenesis of *Nasonia vitripennis* through ovarian delivery of CRISPR-Cas9 ribonucleoprotein. Insect Mol. Biol. 29, 569‑577. https://doi.org/10.1111/imb.12663

Daimon, T., Uchibori, M., Nakao, H., Sezutsu, H., Shinoda, T., 2015. Knockout silkworms reveal a dispensable role for juvenile hormones in holometabolous life cycle. Proc. Natl. Acad. Sci. 112, E4226–E4235. https://doi.org/10.1073/pnas.1506645112

Dermauw, W., Jonckheere, W., Riga, M., Livadaras, I., Vontas, J., Van Leeuwen, T., 2020. Targeted mutagenesis using CRISPR-Cas9 in the chelicerate herbivore *Tetranychus urticae*. Insect Biochem. Mol. Biol. 120, 103347. https://doi.org/10.1016/j.ibmb.2020.103347

Gantz, V.M., Akbari, O.S., 2018. Gene editing technologies and applications for insects. Curr. Opin. Insect Sci. 28, 66–72. https://doi.org/10.1016/j.cois.2018.05.006

Heu, C.C., McCullough, F.M., Luan, J., Rasgon, J.L., 2020. CRISPR-Cas9-based genome editing in the silverleaf whitefly (*Bemisia tabaci*). CRISPR J. 3, 89–96. https://doi.org/10.1089/crispr.2019.0067

Hwang, W.Y., Fu, Y., Reyon, D., Maeder, M.L., Tsai, S.Q., Sander, J.D., Peterson, R.T., Yeh, J.R.J., Joung, J.K., 2013. Efficient genome editing in zebrafish using a CRISPR-Cas system. Nat. Biotechnol. 31, 227–229. https://doi.org/10.1038/nbt.2501

Koller, C.N.., Dhadialla, T.S., Raikhel, A.S., 1989. Selective endocytosis of vitellogenin by oocytes of the mosquito, *Aedes aegypti*: An in vitro study. Insect Biochem. 19, 693–702. https://doi.org/10.1016/0020-1790(89)90106-6

Koller, C.N., Raikhel, A.S., 1991. Initiation of vitellogenin uptake and protein synthesis in the mosquito (*Aedes aegypti*) ovary in response to a blood meal. J. Insect Physiol. 37,

703–711. https://doi.org/10.1016/0022-1910(91)90048-5

Li, X., Xu, Y., Zhang, H., Yin, H., Zhou, D., Sun, Y., Ma, L., Shen, B., Zhu, C., 2021. ReMOT Control delivery of CRISPR-Cas9 ribonucleoprotein complex to induce germline mutagenesis in the disease vector mosquitoes *Culex pipiens pallens* (Diptera: Culicidae). J. Med. Entomol. 58, 1202–1209. https://doi.org/10.1093/jme/tjab016

Macias, V.M., McKeand, S., Chaverra-Rodriguez, D., Hughes, G.L., Fazekas, A., Pujhari, S., Jasinskiene, N., James, A.A., Rasgon, J.L., 2020. Cas9-mediated gene-editing in the malaria mosquito *Anopheles stephensi* by ReMOT Control. G3 Genes, Genomes, Genet. 10, 1353–1360. https://doi.org/10.1534/g3.120.401133

Matthews, B.J., Vosshall, L.B., 2020. How to turn an organism into a model organism in 10 "easy" steps. J. Exp. Biol. 223, jeb218198. https://doi.org/10.1242/jeb.218198

Mclaughlin, J.M., Bratu, D.P., 2015. *Drosophila melanogaster* Oogenesis: An Overview. Methods Mol. Biol. 1328, 1–20. https://doi.org/10.1007/978-1-4939-2851-4_1

Raikhel, A.S., Dhadialla, T.S., 1992. Accumulation of yolk proteins in insect oocytes. Annu. Rev. Entomol. 37, 217–251. https://doi.org/10.1146/annurev.ento.37.1.217

Sharma, A., Pham, M.N., Reyes, J.B., Chana, R., Yim, W.C., Heu, C.C., Kim, D., Chaverra-Rodriguez, D., Rasgon, J.L., Harrell, R.A., Nuss, A.B., Gulia-Nuss, M., 2022. Cas9-mediated gene editing in the black-legged tick, *Ixodes scapularis*, by embryo injection and ReMOT Control. iScience 25, 103781. https://doi.org/10.1016/j.isci.2022.103781

Shirai, Y., Daimon, T., 2020. Mutations in *cardinal* are responsible for the *red-1* and *peach* eye color mutants of the red flour beetle *Tribolium castaneum*. Biochem. Biophys. Res. Commun. 529, 372–378. https://doi.org/10.1016/j.bbrc.2020.05.214

Shirai, Y., Piulachs, M.-D., Belles, X., Daimon, T., 2022. DIPA-CRISPR is a simple and accessible method for insect gene editing. Cell Rep. Methods 2, 100215.

https://doi.org/10.1016/j.crmeth.2022.100215

Chapter 5
General Discussion

Rapidly evolving genome editing technology has enabled utilization of sophisticated genome engineering in a wide variety of organisms. In insects, genome editing has traditionally been conducted via the microinjection of materials into fertilized eggs. However, this approach is difficult as it requires sophisticated techniques, expensive equipment, and species-specific optimization. Furthermore, microinjection into early embryos can be challenging in some insect species due to their unique biological characteristics. Recently, the Receptor-Mediated Ovary Transduction of Cargo (ReMOT) method has been developed as an alternative to difficult embryonic microinjection (Chaverra-Rodriguez et al., 2018). In this technology, the injection of materials into adult females introduces heritable mutations in their offspring. Initially developed in the yellow fever mosquito *Aedes aegypti*, ReMOT technology facilitates the translocation of the RNP complex into developing oocytes by fusion of a peptide ligand called P2C, derived from *Drosophila* yolk protein1, with the Cas9 protein.

I tested whether ReMOT could be applied to the red flour beetle *T. castaneum*, using the *Drosophila* ligand P2C (Chapter 2). Then, I successfully demonstrated ReMOT-mediated targeted mutagenesis in the beetle, although the efficiency was relatively low. Around the same time, several research papers reported the applicability of ReMOT to various insect species, including mosquitoes, whiteflies, and wasps (Chaverra-Rodriguez et al., 2020; Heu et al., 2020; Macias et al., 2020). In the whitefly, *Bemisia tabaci*, the P2C ligand showed lower efficiency compared to that in mosquitoes. Consequently, the authors developed a novel vitellogenin-based ligand named BtKV (13 amino acids), which was significant and promising because vitellogenin is widely conserved in arthropods and oviparous vertebrates.

However, it was also revealed that ReMOT requires optimization of a ligand tag to achieve successful results in particular species. These procedures require multiple steps, which include vector cloning and protein expression and purification, which can be laborious and challenging for non-specialists. In my study, I conducted ReMOT experiments in *T. castaneum* to pursue further improvements in efficiency using P2C-Cas9. Although I tested various experimental conditions, such as the stage of adults and the concentration of endosomal escape reagents (EERs), I was unable to recover a single mutant from more than 1,000 injected adults (data not shown). For example, I did not recover any mutants from day 4 females injected with in-house P2C-Cas9 (data not shown). However, when I switched to commercial Cas9 (i.e., DIPA-CRISPR), significant number of mutants from same-stage females were obtained. Given that the same colony and the same sgRNA were used, the results suggest that the P2C-Cas9 produced and purified in my lab does not work for the adult injection approach. I must recognize that my laboratory is not familiar with protein expression and purification, thus, the quality of my in-house Cas9 may not be high enough for adult injection. This may also be a problem in other laboratories.

Compared to ReMOT, DIPA-CRISPR is simpler technique as it allows the direct use of commercially available Cas9. In Chapter 3, I demonstrated that the injection of commercial Cas9 and sgRNA can achieve highly efficient genome editing in two different insect species: the German cockroach *B. germanica* and the beetle *T. castaneum*. Notably, the genome editing efficiency reached approximately 20% and exceeded 50% in *B. germanica* and *T. castaneum*, respectively. These efficiencies are relatively high compared to those reported in previous ReMOT studies, although direct comparisons cannot be made. Moreover, I demonstrated that DIPA-CRISPR can be applied to the yellow fever mosquito *A. aegypti* (Chapter 4). These three insect species have different types of ovaries (i.e., panoistic, telotrophic meroistic, and polytrophic meroistic) (Mclaughlin and Bratu, 2015), highlighting

the versatility of this method.

As reported in most biochemistry studies (Nishimasu et al., 2014; Anders et al., 2014), Cas9 is purified by a combination of affinity chromatography and ion-exchange chromatography or/and size-exclusion chromatography. However, in previous ReMOT studies, Cas9 was purified using a single step of affinity chromatography, which could result in contamination with undesired materials. I believe that use of high-quality Cas9 is the key factor for efficient genome editing by adult injection. This view is further supported by my finding that commercial Cas9 products from other companies work for DIPA-CRISPR with similar efficiency (Fig. 3.6A). It would be meaningful to test company-made and biochemistry lab-made Cas9 fused with a ligand peptide. Recently, collaborative research with a biochemistry laboratory helped me in successfully establishing a Cas9 purification procedure in my laboratory. Notably, I demonstrated that the efficiency of this lab-made "naked" Cas9 was comparable to that of commercial Cas9. The original DIPA-CRISPR method uses a commercial Cas9, which hinders its application in large species due to the increasing cost of reagents. The lab-made Cas9 resolves the cost issue and paves the way for further rational engineering of Cas9, suggesting further increase in the efficiency and versatility of the DIPA-CRISPR approach. Currently, I am exploring whether the fusion of the P2C ligand or a vitellogenin-based ligand can enhance the genome editing efficiency (Shirai et al., in preparation).

Significantly, DIPA-CRISPR enables simple and efficient targeted mutagenesis along with achieving targeted gene knock-in via a homology-directed repair (HDR) pathway, as demonstrated in Chapter 3. It was surprising to find that co-injection of a Cas9 RNP complex and ssODNs as a donor template can lead to HDR-mediated gene knock-in events, even though the knock-in efficiency was relatively low. In the adult injection approach, the primary challenge for targeted gene knock-in is the delivery of donor DNA templates, such as

ssODNs, dsDNAs, and plasmids, into oocytes. Recently, Aird et al. (2018) revealed that covalent attachment of ssODN to an engineered Cas9 fused with a HUH endonuclease (i.e., porcine circovirus 2 (PCV2) Rep protein) enhanced the efficiency of HDR-mediated targeted gene knock-in in cell culture. To test whether this method can improve the knock-in efficiency in insects, I used lab-made PCV-Cas9 that was purified using latest procedure developed by me and demonstrated a significant improvement of knock-in efficiency (Shirai et al., in preparation). For the integration of larger DNA fragments, Han et al. (2023) demonstrated that tethering 3′-overhang dsDNA donors with 3′-extended sgRNA (i.e., esgRNA) could improve the knock-in efficiency. Combining these approaches with DIPA-CRISPR could enable us to perform more sophisticated genome engineering in insects.

Since the discovery of ReMOT in 2018 (Chaverra-Rodriguez et al., 2018), the adult injection approach of genome editing has been successfully applied to a diverse range of arthropods, including mosquitoes (Li et al., 2021; Macias et al., 2020; Shirai et al., 2023; Yang et al., 2023), moths (Yu et al., 2023), beetles (Shirai et al., 2022; Shirai and Daimon, 2020), wasps (Chaverra-Rodriguez et al., 2020), whiteflies (Heu et al., 2020), psyllids (Chaverra-Rodriguez et al., 2023), kissing bugs (Lima et al., 2023), stink bugs (Terradas et al., 2023), thrips (De Rouck et al., 2024), planthoppers (Zhang et al., 2023), cockroaches (Shirai et al., 2022), and non-insect arthropods (Dermauw et al., 2020; De Rouck et al., 2024; Sharma et al., 2022) (listed in Table 5.1). The adult injection approach has attracted the attention of many researchers as it does not require embryonic microinjection. In principle, its application could potentially be extended to other arthropod chelicerates (mites and spiders) and crustaceans (shrimp and crabs). In the freshwater prawn *Macrobrachium rosenbergii*, the fusion of a vitellogenin-based peptide ligand named VgP with dsRNA facilitated their translocation into the ovary (Cohen et al., 2023), suggesting that the VgP ligand is a promising method for future genome editing via adult injection in crustaceans. I hope the

adult injection approach can be further expanded to many types of animals, revolutionizing the research in emerging model organisms across many fields.

Class	Order	Species	Target gene	Method	Parental cross (injected females x males)	G_0 screening	Cas9	Highest GEF	Reference	Comments
Insecta	Diptera	*Aedes aegypti*	*kmo/cinnabar*	ReMOT	wt x mutant	phenotype	P2C-Cas9	2.4%	Chaverra-Rodriguez et al. 2013 Nat. commun	Table 1, 25 out of 1052 G_0
			kmo/cinnabar	ReMOT	wt x mutant	phenotype	P2C-EGFP-Cas9	1.1%	Chaverra-Rodriguez et al. 2013 Nat. commun	Table 1, 6 out of 534 G_0
			kmo/cinnabar	ReMOT	wt x wt	phenotype	P2C-EGFP-Cas9	0.07%	Chaverra-Rodriguez et al. 2013 Nat. commun	Table 1, 1 out of 1413 G_0
			kmo/cinnabar	DIPA-CRISPR	wt x wt	PCR/HMA	commercial Cas9 (IDT, V3)	3.5%	Shirai et al. 2023 Appl. Entomol. Zool.	Table 1, 10 out of 288 G_0
		Anopheles stephensi	*enhanced cyan fluorescent protein* (*ecfp*)	ReMOT	TG (ecfp) x wt	phenotype	P2C-Cas9	5.7%	Macias et al. 2020 G3	Table 1, 11 out of 194 G0
		Anopheles sinensis	*kmo/cinnabar*	ReMOT	wt x wt	phenotype (X-linked)	P2C-Cas9	13.6%	Yang et al. 2023 Insect Sci.	Table S3, 434 out of 3198 G_0
			kmo/cinnabar	ReMOT	wt x mutant	phenotype (X-linked)	P2C-Cas9	33.4%	Yang et al. 2023 Insect Sci.	Table S6, 1924 out of 5763 G_0
			yellow	ReMOT	wt x wt	phenotype (X-linked)	P2C-Cas9	0.67%	Yang et al. 2023 Insect Sci.	Table S5, 56 out of 8324 G_0
			yellow	ReMOT	wt x mutant	phenotype (X-linked)	P2C-Cas9	3.9%	Yang et al. 2023 Insect Sci.	Table S7, 99 out of 2562 G_0
		Culex pipiens	*kmo/cinnabar*	ReMOT	wt x wt	phenotype	P2C-Cas9	0.40%	Li et al. 2021 J. Med. Entomol.	Table 4, 9 out of 2251 G_0
	Lepidoptera	*Bombyx mori*	*BLOS2*	ReMOT	wt x wt	phenotype (Z-linked)	OTP-Cas9	NA	Yu et al. 2023 Insects	Table 1, 2 out of 16 injected females
	Coleoptera	*Tribolium castaneum*	*cardinal*	ReMOT	wt x wt	phenotype (X-linked)	P2C-Cas9	0.26%	Shirai and Daimon. 2020 BBRC	Fig. 3, 1 out of 383 G_0
			cardinal	DIPA-CRISPR	wt x wt	phenotype (X-linked)	commercial Cas9 (IDT, V3)	71.4%	Shirai et al. 2022 Cell Rep. Methods	Fig. 3, 17 out of 54 G_0, Successful knock-in
	Hymenoptera	*Nasonia vitripennis*	*kmo/cinnabar*	ReMOT	not crossed (arrhenotoky)	phenotype (haplodiploid)	P2C-Cas9-EGFP	0.61%	Chaverra-Rodriguez et al. 2020 Insect Mol. Biol.	Table 1, 9 out of 1471 G_0
			kmo/cinnabar	ReMOT	not crossed (arrhenotoky)	phenotype (haplodiploid)	P2C-Cas9	0.33%	Chaverra-Rodriguez et al. 2020 Insect Mol. Biol.	Table 1, 4 out of 1229 G_0
			kmo/cinnabar	DIPA-CRISPR/BAPC (DIPA + BAPC)	not crossed (arrhenotoky)	phenotype (haplodiploid)	commercial Cas9 (PNA Bio, CP01)	0.85%	Chaverra-Rodriguez et al. 2020 Insect Mol. Biol.	Table 1, 8 out of 943 G_0
	Hemiptera	*Bemisia tabaci*	*white*	ReMOT	wt x wt	phenotype (haplodiploid)	BtKV-Cas9	12.7%	Heu et al. 2020 CRISPR J	Table 1, 15 out of 118 G_0
		Diaphorina citri	*white*	ReMOT	wt x wt	phenotype	P2C-Cas9	3.6%	Chaverra-Rodriguez et al. 2023 GEN Biotechnol.	Table 2, 1 out of 28 G_0
			white	DIPA-CRISPR	wt x wt	phenotype	commercial Cas9 (PNA Bio)	8.8%	Chaverra-Rodriguez et al. 2023 GEN Biotechnol.	Table 2, 12 out of 136 G_0
		Halyomorpha halys	*kmo/cinnabar*	ReMOT	wt x wt	phenotype	P2C-Cas9	2.1%	Terradas et al. 2022 Transgenic Insects 2nd Edition, Chapter 6	Section 6.5.2, 4 out of 194 G_0
		Orius strigicollis	*cinnabar*	DIPA-CRISPR	wt x wt	PCR/HMA	commercial Cas9 (IDT, V3)	~30%	Matsuda et al. in prep.	NA
		Plautia stali	*cinnabar*	DIPA-CRISPR	wt x wt	PCR/HMA	commercial Cas9 (IDT, V3)	42.4%	Takahashi et al. in prep.	NA
		Rhodnius prolixus	*yellow*	ReMOT	wt x wt	phenotype	BtKV-Cas9	0.68%	Lima et al. 2023 bioRxiv	Table 1, 1 out of 148 G_0
			scarlet	ReMOT	wt x wt	phenotype	BtKV-Cas9	0.74%	Lima et al. 2023 bioRxiv	Table 1, 1 out of 135 G_0
			white	ReMOT	wt x wt	phenotype	BtKV-Cas9	0.70%	Lima et al. 2023 bioRxiv	Table 1, 1 out of 142 G_0
			yellow, scarlet, white, aaNAT (a mixture of 4 gRNAs)	ReMOT	wt x wt	phenotype	BtKV-Cas9	4.0%	Lima et al. 2023 bioRxiv	Table 1, 3 out of 80 G_0
		Sogatella furcifera	*vermilion/tryptophan 2,3-dioxygegeriase*	DIPA-CRISPR	wt x wt	phenotype	commercial Cas9 (PNA Bio, CP02)	56.7%	Zhang et al., 2023 Insect Sci.	Table 1, 55 out of 97 G_0
	Tysanoptera	*Frankliniella occidentalis*	*white*	DIPA-CRISPR/SYNCAS (DIPA + EER +BAPC)	not crossed (arrhenotoky)	phenotype (haplodiploid)	commercial Cas9 (IDT, V3)	30.4%	De Rouck et al. 2024 Insect Biochem. Mol. Biol.	Table 3, 21 out of 69 G_0 Successful knock-in
			white-like	DIPA-CRISPR/SYNCAS (DIPA + EER +BAPC)	not crossed (arrhenotoky)	phenotype (haplodiploid)	commercial Cas9 (IDT, V3)	32.1%	De Rouck et al. 2024 Insect Biochem. Mol. Biol.	Table 3, 25 out of 78 G_0
	Blattodea	*Blattella germanica*	*cinnabar*	DIPA-CRISPR	wt x wt	PCR/HMA	commercial Cas9 (IDT, V3)	21.8%	Shirai et al. 2022 Cell Rep. Methods	Fig. 1, 57 out of 215 G_0
Arachnida	Trombidiformes	*Tetranychus urticae*	*phytoene desaturase*	DIPA-CRISPR	not crossed (arrhenotoky)	phenotype (haplodiploid)	commercial Cas9 (IDT, V3)	0.38%	Dermauw et al. 2020 Insect Biochem. Mol. Biol.	Section 3.2.1, 1 out of 260 G_0
			phytoene desaturase	DIPA-CRISPR/SYNCAS (DIPA + EER + BAPC)	not crossed (arrhenotoky)	phenotype (haplodiploid)	commercial Cas9 (IDT, V3)	24.4%	De Rouck et al. 2024 Insect Biochem. Mol. Biol.	Table S7, 10 out of 41 G_0 Successful knock-in
			CYP384A1	DIPA-CRISPR/SYNCAS (DIPA + EER + BAPC)	not crossed (arrhenotoky)	phenotype (haplodiploid)	commercial Cas9 (IDT, V3)	17.7%	De Rouck et al. 2024 Insect Biochem. Mol. Biol.	Table S7, 12 out of 68 G_0
			Antennapedia	DIPA-CRISPR/SYNCAS (DIPA + EER + BAPC)	not crossed (arrhenotoky)	phenotype (haplodiploid)	commercial Cas9 (IDT, V3)	13.8%	De Rouck et al. 2024 Insect Biochem. Mol. Biol.	Table S7, 8 out of 58 G_0
	Ixodida	*Ixodes scapularis*	*Proboscepedia*	ReMOT	wt x wt	PCR/Sanger sequencing	P2C-Cas9	4.2%	Sharma et al. 2022 iScience	Table 1, 7 out of 168 G_0

Table. 5.1. List of successful results of genome editing by adult injection in arthropods

References

Aird, E.J., Lovendahl, K.N., St. Martin, A., Harris, R.S., Gordon, W.R., 2018. Increasing Cas9-mediated homology-directed repair efficiency through covalent tethering of DNA repair template. Commun. Biol. 1, 54. https://doi.org/10.1038/s42003-018-0054-2

Anders, C., Niewoenher, O., Duerst, A., Jinek, M., 2014. Structural basis of PAM-dependent target DNA recognition by the Cas9 endonuclease. Nature 513, 569–573. https://doi.org/10.1038/nature13579

Chaverra-Rodriguez, D., Bui, M., Gilleland, C.L., Rasgon, J.L., Akbari, O.S., 2023. CRISPR/Cas9-mediated mutagenesis of the Asian Citrus Psyllid, *Diaphorina citri*. GEN Biotechnol. 2, 2023.05.05.539615. https://doi.org/10.1089/genbio.2023.0022

Chaverra-Rodriguez, D., Macias, V.M., Hughes, G.L., Pujhari, S., Suzuki, Y., Peterson, D.R., Kim, D., McKeand, S., Rasgon, J.L., 2018. Targeted delivery of CRISPR-Cas9 ribonucleoprotein into arthropod ovaries for heritable germline gene editing. Nat. Commun. 9, 1–11. https://doi.org/10.1038/s41467-018-05425-9

Chaverra-Rodriguez, D., Dalla Benetta, E., Heu, C.C., Rasgon, J.L., Ferree, P.M., Akbari, O.S., 2020. Germline mutagenesis of *Nasonia vitripennis* through ovarian delivery of CRISPR-Cas9 ribonucleoprotein. Insect Mol. Biol. 29, 569–577. https://doi.org/10.1111/imb.12663

Cohen, S., Hasan, M., Frishman, N., Khalaila I., 2023. A crustacean vitellogenin-derived peptide as an oocyte-specific delivery vehicle for gene silencing. Front. Mar. Sci. 10, 1128524. https://doi.org/10.3389/fmars.2023.1128524

Dermauw, W., Jonckheere, W., Riga, M., Livadaras, I., Vontas, J., Van Leeuwen, T., 2020. Targeted mutagenesis using CRISPR-Cas9 in the chelicerate herbivore *Tetranychus*

urticae. Insect Biochem. Mol. Biol. 120, 103347. https://doi.org/10.1016/j.ibmb.2020.103347

De Rouck, S., Mocchetti, A., Dermauw, W., Van Leeuwen, T., 2024. SYNCAS: Efficient CRISPR/Cas9 gene-editing in difficult to transform arthropods. Insect Biochem. Mol. Biol. 165, 104068. https://doi.org/10.1016/j.ibmb.2023.104068

Han, W., Li, Z., Guo, Y., He, K., Li, W., Xu, C., Ge, L., He, M., Yin, X., Zhou, J., Li, C., Yao, D., Bao, J., Liang, H., 2023. Efficient precise integration of large DNA sequences with 3'-overhang dsDNA donors using CRISPR/Cas9. Proc. Natl. Acad. Sci. 120, e2221127120. https://doi.org/10.1073/pnas.2221127120

Heu, C.C., McCullough, F.M., Luan, J., Rasgon, J.L., 2020. CRISPR-Cas9-based genome editing in the silverleaf whitefly (*Bemisia tabaci*). Cris. J. 3, 89–96. https://doi.org/10.1089/crispr.2019.0067

Li, X., Xu, Y., Zhang, H., Yin, H., Zhou, D., Sun, Y., Ma, L., Shen, B., Zhu, C., 2021. ReMOT Control delivery of CRISPR-Cas9 ribonucleoprotein complex to induce germline mutagenesis in the disease vector mosquitoes *Culex pipiens pallens* (Diptera: Culicidae). J. Med. Entomol. 58, 1202–1209. https://doi.org/10.1093/jme/tjab016

Lima, L., Berni, M., Mota, J., Bressan, D., Julio, A., Cavalcante, R., Macias, V., Li, Z., Rasgon, J.L., Bier, E., Araujo, H., 2023. Gene editing in the Chagas disease vector *Rhodnius prolixus* by Cas9-mediated ReMOT Control. bioRxiv https://doi.org/10.1101/2023.08.14.553172.

Macias, V.M., McKeand, S., Chaverra-Rodriguez, D., Hughes, G.L., Fazekas, A., Pujhari, S., Jasinskiene, N., James, A.A., Rasgon, J.L., 2020. Cas9-mediated gene-editing in the malaria mosquito *Anopheles stephensi* by ReMOT Control. G3 Genes, Genomes, Genet. 10, 1353–1360. https://doi.org/10.1534/g3.120.401133

Mclaughlin, J.M., Bratu, D.P., 2015. *Drosophila melanogaster* Oogenesis: An Overview.

Methods Mol. Biol. 1328, 1–20. https://doi.org/10.1007/978-1-4939-2851-4_1

Nishimasu, H., Ran, F.A., Hsu, P.D., Konermann, S., Shehata, S.I., Dohmae, N., Ishitani, R., Zhang, F., Nureki, O., 2014. Crystal structure of Cas9 in complex with guide RNA and target DNA. Cell 156, 935–949. https://doi.org/10.1016/j.cell.2014.02.001

Sharma, A., Pham, M.N., Reyes, J.B., Chana, R., Yim, W.C., Heu, C.C., Kim, D., Chaverra-Rodriguez, D., Rasgon, J.L., Harrell, R.A., Nuss, A.B., Gulia-Nuss, M., 2022. Cas9-mediated gene editing in the black-legged tick, *Ixodes scapularis*, by embryo injection and ReMOT Control. iScience 25, 103781. https://doi.org/10.1016/j.isci.2022.103781

Shirai, Y., Daimon, T., 2020. Mutations in *cardinal* are responsible for the *red-1* and *peach* eye color mutants of the red flour beetle *Tribolium castaneum*. Biochem. Biophys. Res. Commun. 529, 372–378. https://doi.org/10.1016/j.bbrc.2020.05.214

Shirai, Y., Piulachs, M.-D., Belles, X., Daimon, T., 2022. DIPA-CRISPR is a simple and accessible method for insect gene editing. Cell Rep. Methods 2, 100215. https://doi.org/10.1016/j.crmeth.2022.100215

Shirai, Y., Takahashi, M., Ote, M., Kanuka, H., Daimon, T., 2023. DIPA-CRISPR gene editing in the yellow fever mosquito *Aedes aegypti* (Diptera: Culicidae). Appl. Entomol. Zool. 58, 273–278. https://doi.org/10.1007/s13355-023-00831-y

Terradas, G., Macias, V.M., Peterson, H., McKeand, S., Krawczyk, G., Rasgon, J.L., 2022. Chapter 6: Receptor-Mediated Ovary Transduction of Cargo - ReMOT Control: a Comprehensive Review and Detailed Protocol for Implementation. Transgenic Insects: Techniques and Applications. 2nd Edition (CABI Books), 125–148.

Yang, X.L., Ling, X., Sun, Q., Qiu, P.P., Xiang, K., Hong, J.F., He, S.L., Chen, J., Ding, X., Hu, H., He, Z.B., Zhou, C., Chen, B., Qiao, L., 2023. High-efficiency gene editing in *Anopheles sinensis* using ReMOT control. Insect Sci.

https://doi.org/10.1111/1744-7917.13306

Yu, B., Dong, S., Jiang, X., Qiao, L., Chen, J., Li, T., Pan, G., Zhou, Z., Li, C., 2023. Cas9-mediated gene editing using Receptor-Mediated Ovary Transduction of Cargo (ReMOT) Control in *Bombyx mori*. Insects 14, 932. https://doi.org/10.3390/insects14120932

Zhang, M.Q., Gong, L.L., Zhao, Y.Q., Ma, Y.F., Long, G.J., Guo, H., Liu, X.Z., Hull, J.J., Dewer, Y., Yang, C., Zhang, N.N., He, M., He, P., 2023. Efficient DIPA-CRISPR-mediated knockout of an eye pigment gene in the white-backed planthopper, *Sogatella furcifera*. Insect Sci. https://doi.org/10.1111/1744-7917.13286

Acknowledgments

I would like to express my deepest gratitude to all those who have contributed to the completion of this doctoral thesis.

First and foremost, I am deeply grateful to my supervisor, Dr. Takaaki Daimon, Division of Applied Biosciences, Graduate School of Agriculture, Kyoto University, for his unwavering support, invaluable guidance, and constant encouragement throughout the course of my research. I would also like to convey my deep thanks to Dr. Takahiro Ohde, Dr. Toshiya Ando, Dr. Naoki Matsuda, and the members of the Laboratory of Insect Physiology, Division of Applied Biosciences, Graduate School of Agriculture, Kyoto University, for their assistance with experiments and stimulating discussions.

I sincerely thank Dr. Yoshitaka Takano and Dr. Kazuyuki Mise, Division of Applied Biosciences, Graduate School of Agriculture, Kyoto University, for their help with protein purification and valuable advice. I am deeply thankful to Dr. Masato Kinoshita, Division of Applied Biosciences, Graduate School of Agriculture, Kyoto University, for sharing information and engaging in productive discussions.

My heartfelt thanks go to Dr. Manabu Ote and Dr. Hirotaka Kanuka, Department of Tropical Medicine, The Jikei University School of Medicine, for their invaluable guidance on mosquito biology. Their research expertise significantly contributed to the success of my project. I would also like to express my warmest thanks to Mr. Ryoya Nakagawa and Dr. Osamu Nureki, Department of Biological Sciences, Graduate School of Science, The University of Tokyo, for their generous assistance. They dedicated two days to instruct me in protein purification and offered valuable advice.

I would be deeply grateful to Dr. Xavier Belles, Dr. Maria-Dolors Piulachs, and Dr.

Jose-Luis Maestro, Institute of Evolutionary Biology, Spain, for their warm welcome and for providing exciting experiences during my 4-month stay. They not only shared a wealth of knowledge about cockroaches but also provided me with abundant insightful advice for my career as a researcher.

In closing, I would like to extend my sincere gratitude to my family for their endless support, encouragement, and understanding throughout my academic pursuit. This work was partially supported by Grant-in-Aid for JSPS Research Fellow (DC1, 21J20658).